FABRICATION OF THIN LAYER POLYMER-BASED BIOINTERPHASE FOR BIOSENSING APPLICATION

A Thesis Submitted to
the Graduate School of Engineering and Sciences of
İzmir Institute of Technology
in Partial Fulfillment of the Requirements for the Degree of

MASTER OF SCIENCE

in Chemistry

by
Müge YÜCEL

July 2016
İZMİR

We approve the thesis of **Müge YÜCEL**

Examining Committee Members:

Assist. Prof. Dr. Ümit Hakan YILDIZ
Department of Chemistry, İzmir Institute of Technology

Prof. Dr. Mustafa M. DEMİR
Department of Materials Science and Engineering, İzmir Institute of Technology

Assist. Prof. Dr. Osman AKIN
Department of Mechatronics Engineering, İzmir Katip Çelebi University

15 July 2016

Assist. Prof. Dr. Ümit Hakan YILDIZ
Supervisor, Department of Chemistry
İzmir Institute of Technology

Prof. Dr. Ahmet Emin EROĞLU
Head of the Department of Chemistry

Prof. Dr. Bilge KARAÇALI
Dean of the Graduate School of Engineering and Science

ACKNOWLEDGEMENT

I would firstly like to thank my thesis advisor Assist. Prof. Dr. Ümit Hakan Yıldız for his guidance and support throughout my thesis study.

I am also thankful to my friends and all Biosens&Bioapps group members for their friendship and encouragement.

I would like to express my special thank to my parents Fatma & Ahmet Yücel, my sisters Özge Ergun and Hilmiye Erk, and also my beloved Gökhan Kaplan for their neverending support and encouragement.

ABSTRACT

FABRICATION OF THIN LAYER POLYMER-BASED BIOINTERPHASE FOR BIOSENSING APPLICATION

This study aims to fabricate polymer-carbon nanotube composite as a bioelectronic interface for sensing volatile organic compounds (VOCs) in exhaled breath. Sensor platform is made of two layers i) polymeric membranes and ii) conducting layer. Poly(vinylidene fluoride) (PVDF), polystyrene (PS), and poly(methyl methacrylate) (PMMA) are selected as model polymers that are processed by electrospinning to utilize polymeric membranes. Multi-walled carbon nanotubes (MWCNTs) are used to fabricate conducting layer on top of PVDF, PS, PMMA polymer membranes. Aqueous solution of well-dispersed MWCNTs are obtained by several purification and filtration steps and conductivity of working MWCNT solution is adjusted about 120 μS/cm for whole study. This solution is further used to impregnate PVDF, PS, PMMA membrane. The PVDF-MWCNT, PS-MWCNT and PMMA-MWCNT sensor platforms are tested by electrochemical station that recording electrical resistivity change by time. All sensors platforms, made of three polymeric membranes-MWCNT, are found to be a responsive upon applying the toluene and acetone vapor. The sensing mechanism is hypothesized as the adsorption of VOCs onto the conducting CNT layer blocking electron stream on CNT network and causing resistivity change. The sensitivity of PVDF-MWCNT sensing platform is exceedingly higher with respect to other two candidates due to solvent vapor- polymeric membrane interactions. This contribution changes sensor platform characteristics and make them quite sensitive to trace amount of VOCs. Acetone and toluene are detected from ppm to ppb range and reproducible responses are recorded. As a result, acetone and toluene, biomarkers of diabetes and lung cancer, can be differentiated with produced sensor.

ÖZET

BİYOSENSÖR UYGULAMALARI İÇİN POLİMERİK İNCE KATMANLI BİYOARAYÜZ ÜRETİMİ

Bu çalışma verilen nefesten uçucu organik bileşikleri algılamaya yönelik biyoelektronik arayüz olarak polimer-karbon nanotüp kompozitleri üretmeyi amaçlamaktadır. Sensor platform iki katmandan oluşmaktadır; i) polimerik zarlar ve ii) iletken katman. Polimerik zarları elektroeğirme metodu ile elde etmek için polivinilidin florür (PVDF), polistiren (PS) ve polimetil metakrilat (PMMA) seçilmiştir. PVDF, PS ve PMMA polimer zarlarının üst yüzeyindeki iletken katman çoklu katmanlı karbon nanotüp (MWCNT) ile sağlanmıştır. Solüsyon içerisinde iyi dağılan karbon nanotüpler birkaç saflaştırma ve filtreleme basamaklarıyla elde edilmiştir ve tüm çalışma için solüsyonun iletkenliği 120 µS/cm değerine ayarlanmıştır. Bu solüsyon daha sonra PVDF, PS ve PMMA zarlarının impregnasyonunda kullanılmıştır. PVDF-MWCNT, PS-MWCNT ve PMMA-MWCNT sensör platformları elektriksel direnç değişimini kaydeden bir elektrokimyasal istasyon ile test edilmiştir. Polimerik zar ve karbon nanotüpten elde edilmiş bütün sensör platformlarının uygulanan aseton ve toluen buharına cevap veren yapıda olduğu gözlemlenmiştir. Algılama mekanizmasının uçucu organik bileşiklerin iletken karbon nanotüp katmanı üzerine adsorpsiyonundan kaynaklandığı varsayılmaktadır böylelikle karbon nanotüp ağındaki elektron akışı engellenir ve direnç değişimi meydana gelir. Çözücü buharı – polimerik zar etkileşimi sebebiyle, PVDF-MWCNT algılayıcı platformunun hassaslığı diğer iki adayın hassaslığına göre oldukça fazladır. Bu katkı sensör platformunun karakteristiğini değiştirerek eser miktardaki uçucu organik bileşiklere hassas hale getirir. ppm ve ppb aralığındaki aseton ve toluen belirlenebilir ve tekrarlanabilir ve güvenilir cevaplar kaydedilir. Sonuç olarak, diyabet ve akciğer kanserinin biyobelirteci olan aseton ve toluen üretilen bu sensörler ile birbirlerinden ayrılabilir.

TABLE OF CONTENTS

LIST OF FIGURES

Figure **Page**

LIST OF TABLES

Figure **Page**

CHAPTER 1

INTRODUCTION

1.1. Scope of the Thesis

Fabrication of polymer-carbon nanotube (CNT) based sensing platform is intended for detection volatile organic compounds (VOCs), acetone and toluene, in exhale breath by conductometric analysis. Effect of both VOCs and type of polymer on response of sensor was investigated. Additionally, sensitivity of each sensor is analyzed in several ppm ranges and their stabilities are also tested. As a further investigation, microfluidic chamber is designed for enhancement of stability and improvement of response.

1.2. Existence of Acetone and Toluene in Breath

Acetone and toluene are two of the most important markers in breath. Acetone is both exogenous and endogenous volatile organic compound. It is formed in cells during some reactions and also entered body with inhaled breath. In healthy breath, the concentration of acetone is in the range of 656 – 836 ppb but it increases to 1000 – 2000 ppb in diabetic breath. On the other hand, toluene is categorized in only exogenous VOCs. Yet it exists in healthy breath with very trace amount, approximately 0.0074 ppb. Impressively, its concentration dramatically rises to 4 – 8 ppb (Konvalina and Haick 2014).

1.2.1. Formation of Ketone Bodies

The molecules, called as ketone bodies, are acetoacetate, D-β-hydroxybutyrate, and acetone. Acetoacetate and D-β-hydroxybutyrate are usually exported to extrahepatic tissues from liver as energy source of various tissues and organs but acetone is exhaled as a toxic molecule.

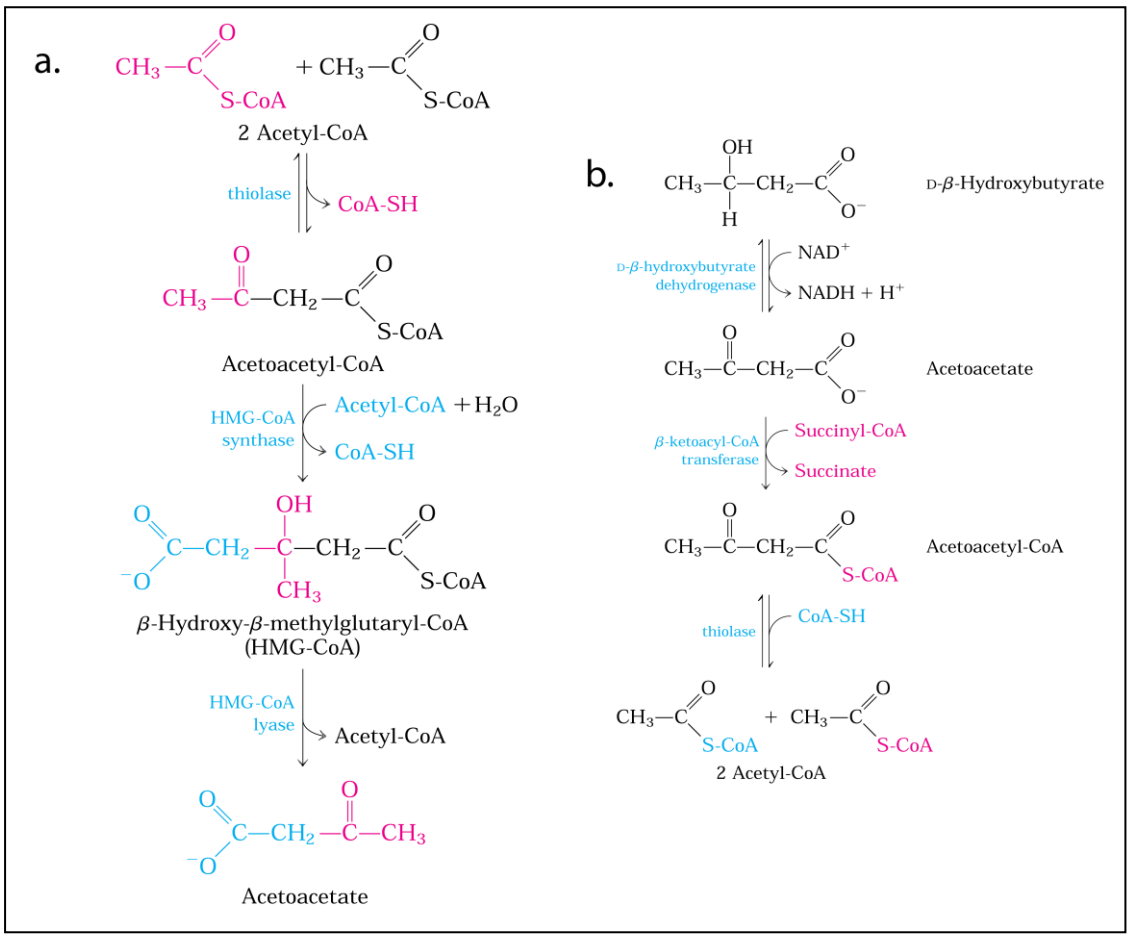

Figure 1.1 Reactions of a) ketone body formation and b) oxidation of D-β hydroxybutyrate

In healthy people, acetone is produced from the reaction (Figure 1.1.a) of acetyl-CoA with a low amount. Acetone has very high volatility property thus can be easily exhaled. The other product of that reaction, D-β-hydroxybutyrate, is then exported to extrahepatic tissues. It is oxidized to form acetyl-CoA with an enzyme-catalyzed reaction (Figure 1.1.b). Acetyl-CoA then enters citric acid cycle to provide energy for body.

In diabetic patients, acetyl-CoA that cannot attend the citric acid cycle is increasingly produced by degradation fatty acids in mitochondria. That increase in amount of acetyl-CoA causes production of excess ketone bodies. Tissues then become insufficient to oxidize all the produced ketone bodies. Therefore; exhalation of acetone will dramatically increase and the level of acetoacetate and D-β-hydroxybutyrate also increases in blood. This apparent increment induces some other changes and then it may cause coma and death.

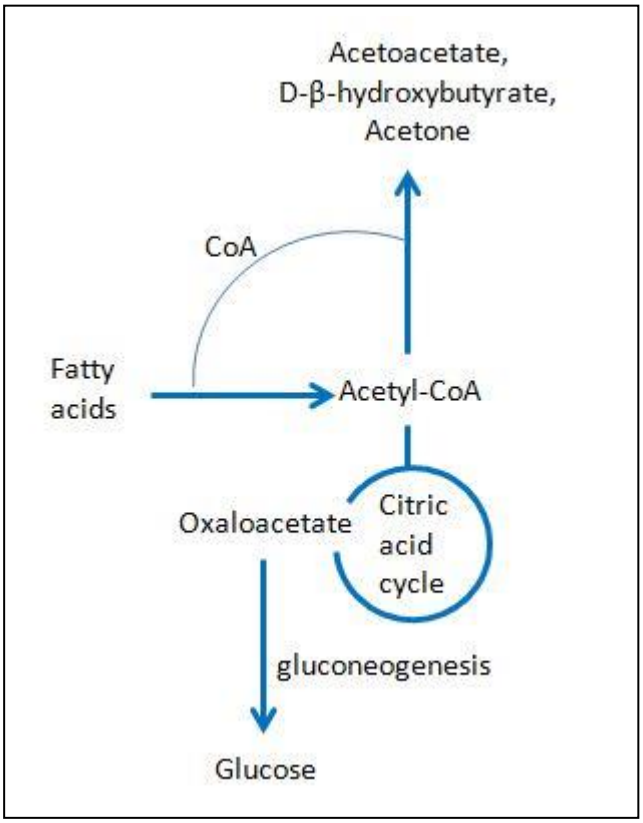

Figure 1.2. Acetyl-CoA in cyclic acid cycle and ketone formation

1.2.2. Role of Aromatic Compounds in Lung Cancer

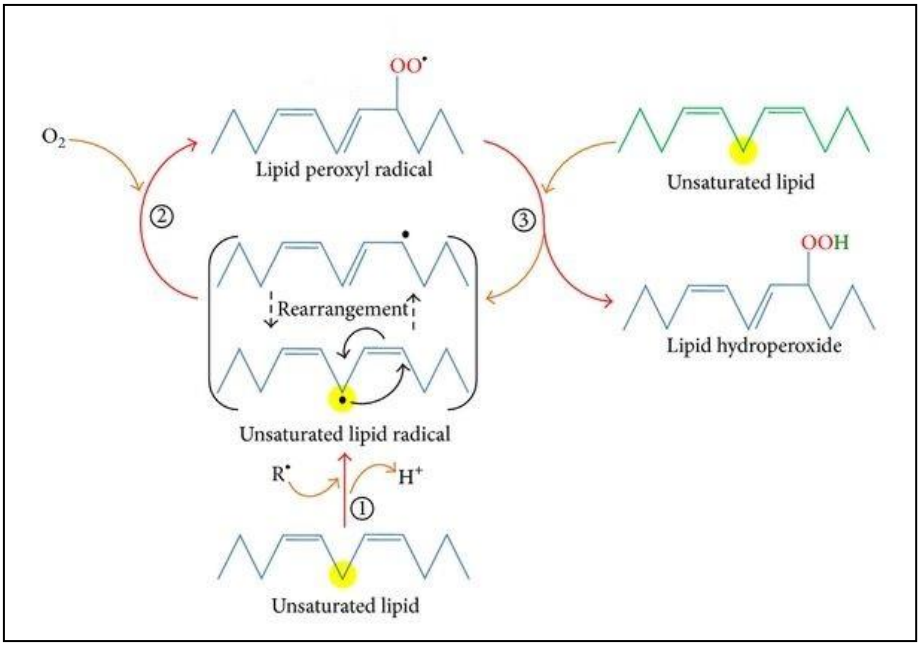

Figure 1.3. Lipid peroxidation process of PUFA (Source: Ayala et al. 2014)

The most abundant aromatic compounds in breath are benzene, styrene, toluene, and 2,5 dimetyl furan. These are exogenously taken to body such as smoking, pollution, and alcohol (Hakim et al. 2012). Accumulation of these molecules in cells increases lipid peroxidation thus they cause damage on proteins, poly unsaturated fatty acid (PUFA), and DNA (Halliwel 1992). Therefore, some severe disease such as cancer occurs.

1.3. Breath Analysis

Breath analysis for detection of diseases is a new generation and promising technique because it is cost effective and non-invasive (Tisch and Haick 2014, Kim, Jahan, and Kabir 2012). There are hundreds of volatile organic compounds (VOCs) in exhaled breath, some of them are significantly biomarkers of various diseases (Poli et al. 2005). Diabetes, asthma, lung cancer, chronic kidney disease, Alzheimer's disease, and auto-immune disease are both noninfectious and infectious diseases being diagnosed with VOCs in exhaled breath (Broza and Haick 2013). VOCs are consist of three sources; i) endogenous (e.g. isoprene), ii) both endogenous and exogenous (e.g. acetone), and iii) exogenous (e.g. toluene) (Broza et al. 2015). There are two major pathways making endogenous VOCs appear in breath; metabolic changes and oxidative stress (Konvalina and Haick 2014). The concentrations of these VOCs are trace amount in breath; however, some sophisticated devices are able to detect low amount of VOCs. The commons techniques are gas chromatography (GC), selected ion flow tube mass spectrometry (SIFT-MS), and proton transfer reaction mass spectrometry (PTR-MS) (Kim et al. 2015).

1.3.1. Gas Chromatography (GC)

Gas chromatography is the most widely used technique to identify volatile compounds in a gas mixture. It is provide both qualitative and quantitative analysis (Wang and Sahay 2009). Gc is a methodology with a characteristic of low limit of detection limit (LOD); it enables analysis of very low amount of analyte. As mentioned above, VOCs exist in exhaled breath at a trace amount, therefore, it makes GC the most suitable technique for breath analysis (Buszewski et al. 2012).

Instrumentation of gas chromatography is shown in figure x. Main components of GC are carrier gas, injection system, chromatographic column, and detection system.

- **carrier gas:** The most common carrier gases used in GC are helium, argon, nitrogen, and hydrogen. Flow rate of the gas is usually controlled by a two-staged pressure regulator at the gas tank.
- **sample injection:** Sample is introduced as a vapor. For an effective separation in column, the size and injection type of sample are significant. Therefore; the injection port should be above boiling point of the least volatile compounds in analyte.
- **chromatographic column:** In GC, column is the part where separation is begun and the most important parameter for separation is temperature. For this reason, column is placed in a thermostatted oven. There are two types of columns: packed and capillary columns. They are differed from each other based on their length.
- **detectors:** There are many detection system used in GC. The detector is chosen depending on the type of sample and the purpose. Main characteristics of the detector are: sensitivity, reproducibility, resistivity to high temperature, a rapid response, etc. However; one type of detector unfortunately cannot have all the characteristics (Skoog, Holler, and Crouch 1998).

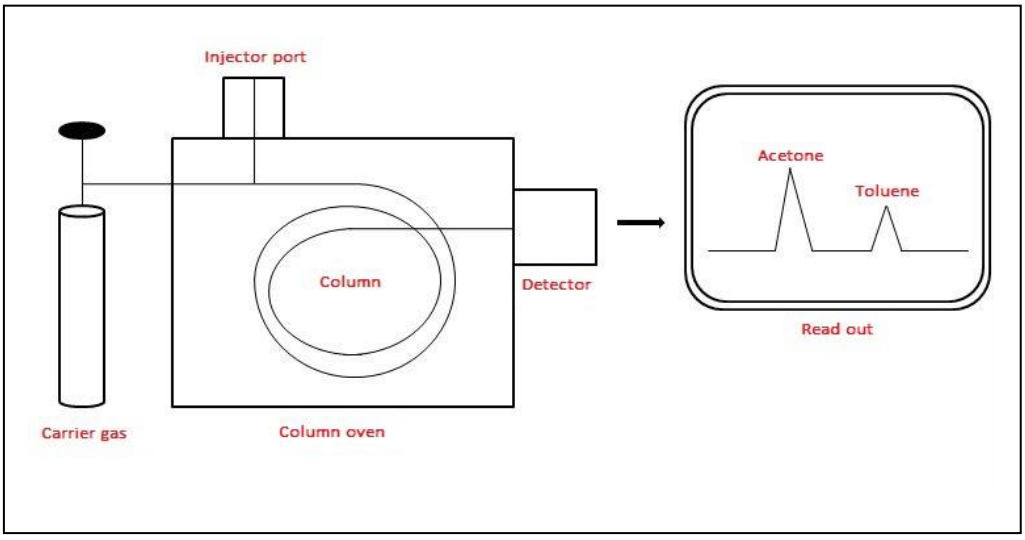

Figure 1.4 Schematic representation of Gas Chromatography (GC)

1.3.2. Selected-Ion Flow Tube/Mass Spectrometry (SIFT/MS)

SIFT/MS is a new quantitative technique which was discovered 40 years ago. The components of SIFT instrument are ion source, injection quadrupole mass filter, carrier gas flow tube reactor, and analytical quadrupole mass spectrometer. Its application is mainly based on biomarkers detection for several diseases. SIFT/MS method is appropriate for VOCs analysis from exhaled breath, it can because detect trace amount sample and work humid media.

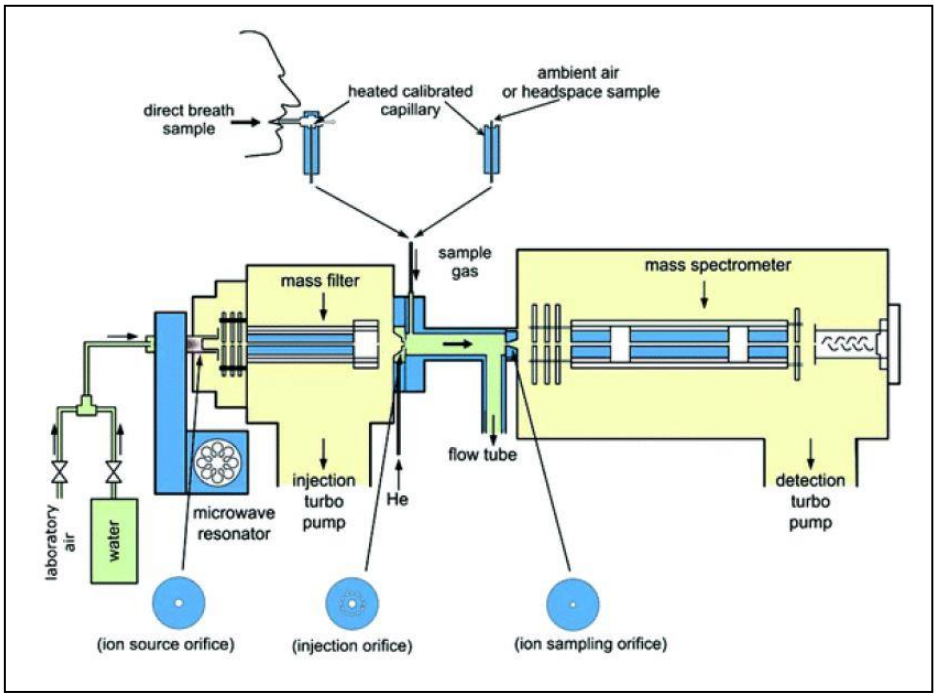

Figure 1.5 Schematic representation of SIFT/MS

These techniques are convenient for breath analysis with respect to properties of components of exhaled breath. However; they are so complex devices that a trained personnel is required. All the constituents of these instruments are quite sophisticated and huge. Therefore a new technique for breath analysis "*nanomaterial-based sensors*" draws attention.

1.3.3. Nanomaterial-Based sensor

For the last decade, nanomaterials are given an enormous attention in the VOC sensors fabrication as in all fields. Materials with nanoscale dimensions, e.g. nanoparticle of various materials and carbon nanotubes, have significant virtue such

as large surface-to-volume ratio and unique chemical, physical, and optical properties with a cost-effective way (Nakhleh et al. 2014). Increasing active surface area of the material makes these sensors very sensitivity as well as rapidly responsive; on the other hand, recovery time decreases (Amann et al. 2014).

1.3. Carbon Nanotubes (CNTs)

Carbon has many allotropes, the most commonly known graphite and diamond. The other examples of carbon nanomaterials are graphene and carbon nanotubes. Graphene is the single layer of graphite. Carbon nanotubes (CNTs) are the rolled up form of graphene. Carbon nanotube is one of the larger materials, the diameter of CNT is several nanometers but its length a few centimeters (Zhang and Baughman 2011). Therefore its excellent electrical, thermal, and mechanical properties makes CNT best candidate for sensor application.

1.4.1. Structure

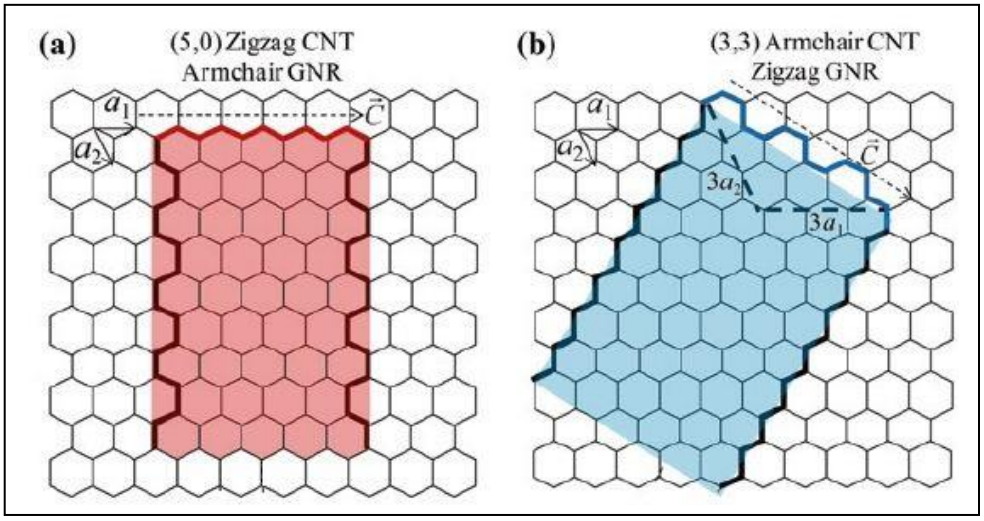

Figure 1.6 Formation of CNT from graphene (Source: Kaushik and Majumder 2015).

Graphene sheet is the 2D honeycomb structure of carbon atoms and its rolling up with different dimensions forms carbon nanotube structures. n_1 and n_2 are the chiral indices which indicates rolling up dimensions of CNT so its zigzag or armchair structures. If n_1 and n_2 are equal, armchair CNTs are formed, when one of the indices

is zero (n_1=0 or n_2=0), zigzag structure of CNTs is formed, and other indices values form chiral structure of CNT (Kaushik and Majumder 2015).

1.4.2. Electrical property

Carbon nanotubes are formed by hexagonal lattice shape of carbon atoms. The all carbon atoms are bonded to each other with sp^2 molecular orbital conformation (Salahuddin, Lundstrom, and Datta 2005). Three electrons on one carbon atom in the structure make sigma bond with adjacent carbon atom and the last valance electron of carbon atom hybridized with that of the other one to form π bond. The perfect delocalization of electron through the π bonds gives electrical conductance (Kittel 1996). However; electrical conductance of carbon nanotubes depends on its rolling up structure. If the chiral indices are equal (armchair), it is totally metallic. When n_1- n_2 is a multiple of 3, it shows semiconducting property. Otherwise, it can be both metallic or semiconducting (Lu and Chen 2005). Conformation of hexagons in carbon nanotubes changes the conductivity. In armchair form, delocalized electrons can easily move conduction band thus armchair nanotubes show greater conductance than metal. However; movement of electron in other conformations is not as easy as much as armchair tubes then they require external power to induce the electrons.

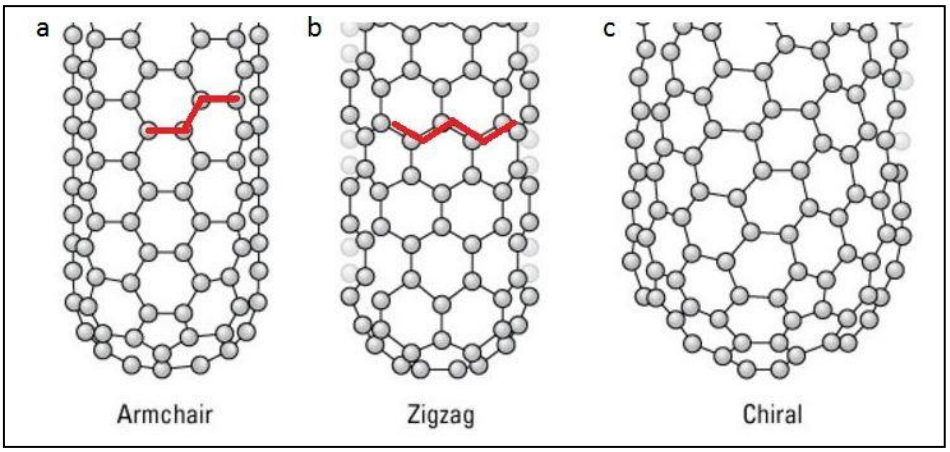

Figure 1.7 Conformation of CNTs a) armchair, b) zigzag, and c) chiral

1.5. Electrospinning

Electrospinning is a technique to get polymer fibers with the diameter range from nanometer to micrometer from its solution or melt. It is attracted a great attention in the past few years in biomedical, material science, and industry areas because of its simplicity and reproducible and continuous fabrication (Greiner and Wendorff 2007). Electrospinning provides fibrous polymers with a variety of size and shape. Nano or micro-sized and homogenous fibers, also porous or film structure of polymer can be controllably obtained (Garg and Bowlin 2011). There are critical parameters for electrospinning process; concentration of solution, nozzle to collector distance, applied voltage, flow rate, temperature, and humidity. However; three of them are major parameters that significantly affect the fabrication; voltage, concentration, and nozzle to collector distance (Magniez, De Lavigne, and Fox 2010).

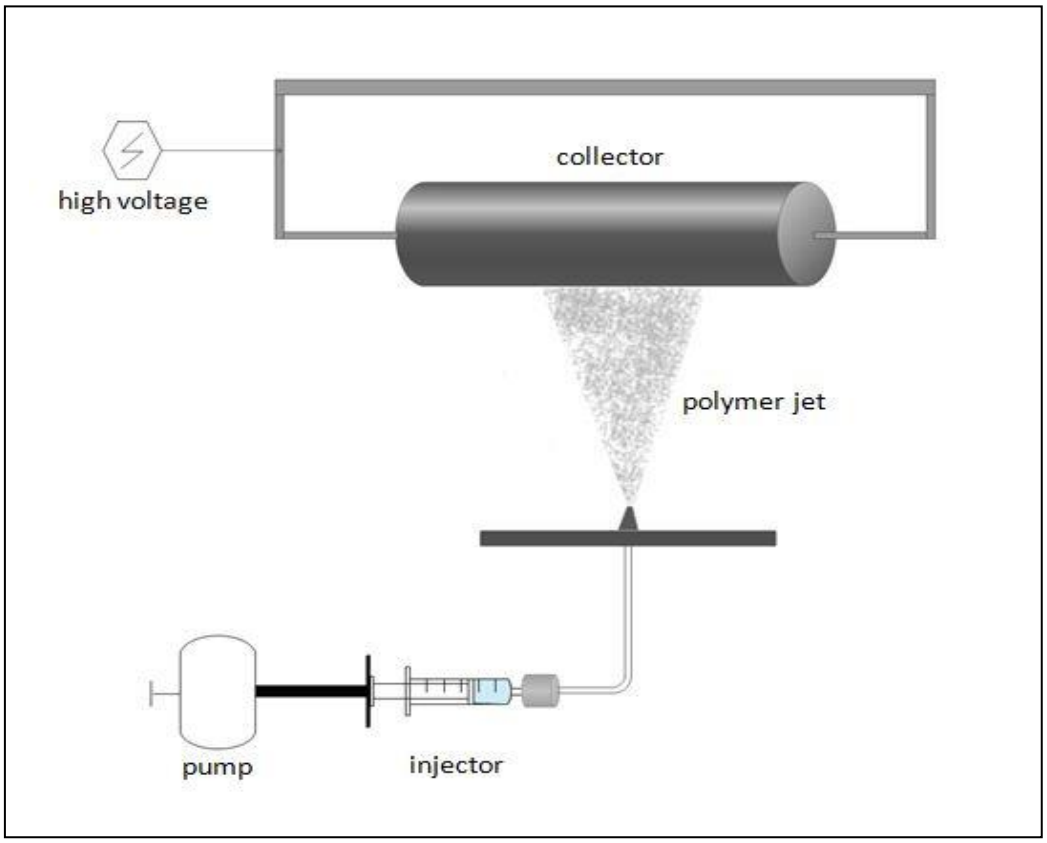

Figure 1.8 Representation electrospinning set-up

A simple electrospinning set-up consists of pump, power source, and conductive collector. a solution of desired product is drawn into a syringe and then it

is placed in a pump connected to the device. Pump provides a certain adjustable flow through the nozzle from syringe. When the solution comes to the nozzle, a drop of solution accumulates at the tip of the nozzle. Afterwards, high electrical field is applied increasingly. Until a critical voltage, the drop can be held by its own surface tension(Zhao et al. 2005). Electrical field electrostatically charges the surface of drop. When the voltage attains the critical value, the liquid drop begins to elongate then transforms into a conical shape. Above that value, electrostatic forces overcome the surface tension of the drop. Liquid polymer solution elongates through the collector meanwhile solvent evaporates (Cozza et al. 2013). Finally solid polymeric fibers are collected.

CHAPTER 2

PREPARATION OF POLYMER-CARBON NANOTUBE (CNT) GAS SENSOR

2.1. Materials & Methods

Poly(vinylidene fluoride) (PVDF; average molecular weight of 275,000, Sigma Aldrich), polystyrene (PS; average molecular weight of 280.000, Sigma Aldrich), and poly(methyl methacrylate) (PMMA; average molecular weight of 350.000, Sigma Aldrich) were utilized for fabrication of polymer fiber. Dimethylformamide (DMF, ≥99.8%), dichloromethane (DCM, ≥99%, Sigma Aldrich), and acetone were used to dissolve polymers. Nitric acid (HNO_3, ≥65%, Sigma Aldrich), Sulfuric acid (H_2SO_4), hydrochloric acid (HCl, ≥37, Sigma Aldrich), and ammonium hydroxide (NH_4OH, 26%, Sigma Aldrich)) were for the functionalization of MWCNTs. Acetone (ACS Rea. Merck) and toluene (ACS Rea. Merck) were used in 2-probe resistivity measurement as VOC vapors.

2.2. Acid Treatment of Carbon Nanotubes

0.1 g MWCNT is weighed and taken into a 50 mL Erlenmeyer. Mixture of 5 mL H2SO4 and 1.7 mL HNO3 solution is then poured onto MWCNTs. This mixture is sonicated for 1 hour. After sonication is finished, it is taken from sonicator and held at fume hood for about 15 hours. 1.7 mL HCl is then added to the solution and shaken slowly. Thereafter, a total 19 mL NH4OH solution is slowly poured to the mixture until the end of the gas releasing in order to neutralize it. After observing pH 7, the solution is filtered with 0.2 micron cellulose acetate filter paper. After that filtration product is taken to a 1 L Erlenmeyer and deionized water is added until making the solution's pH in the range of 5.5 – 6. That solution is again filtered with 0.2 μm porous filter paper. The final product is dried in drying oven for 2 hours at 40^0C.

For the preparation of well-dispersed MWCNT solution, the obtained CNTs are grinded in a mortar. For the preparation of 0.2wt % MWCNT solution, 40 mg is weighed and taken in a 20 mL vial. Then, 20 mL fresh deionized water is added to it. The vial is tightly covered with parafilm and placed into sonicator. The MWCNT solution is sonicated for 4.5 hours but the temperature should not pass through 40^0C. After solution preparation conductivity is measured with pH meter. Conductivity of 0.2wt % MWCNT solution is recorded about 120 μS/cm. From this 0.2wt % stock solution, 5 mL (0.1wt %), 2.5 mL (0.05wt %), 1.25 mL (0.025wt %), and 0.625 mL (0.012wt %) solutions are transferred to other vials and these solutions are fulfilled to 10 mL with deionized water. Conductivities of the 0.1wt %, 0.05wt %, 0.025wt %, and 0.012wt % solutions are again measured as approximately 56, 29, 15, and 9 μS/cm, respectively.

2.3. Fabrication and Impregnation of Fibrous Polymer Mat

Figure 2.1 Electrospinning device (İnovenso Ne300)

For the electrospinning process, poly(vinylidene fluoride) (PVDF), polystyrene (PS), and poly(methyl methacrylate) (PMMA) solutions are prepared.

4.58 g PVDF (25wt %) is weighed in a 20 mL vial. 12 mL dimethylformamide (DMF) and 3 mL acetone are added to PVDF pellets. A magnetic bar is put into the solution and the vial is covered with parafilm. The solution is then placed onto magnetic stirrer with heating. It is stirred overnight at 80^0C and 1200 rpm. After solution is dissolved completely, it drawn into a 20 mL syringe connected to electrospinning set-up. The collector is coated with aluminium foil. The parameters of electrospinning are adjusted as followings; 23 kV voltage, 145 mm nozzle to collector distance, and 3.0 mL/h flow rate. Additionally, both rotation and homogeneity modes of collector are turned on. Then PVDF fiber mat is removed from collector. With the same process PS and PMMA mats are prepared. 2.37 g PS (20wt %) is dissolved in 10 mL DMF and stirred for 4-5 hours at 40^0C and 1200 rpm. The solution is placed into set-up and electrospinning process is begun with the parameters; 25 kV voltage, 3.5 mL/h flow rate, and 210 mm nozzle to collector distance. Electrospinning process lasted for end of the solution with activated rotation and homogeneity mode of collector. After that 1.38 g PMMA (15wt %) is dissolved in 8 mL dichloromethane (DCM), 2 mL DMF, and 2 mL acetone and stirred for 2 hours at 40^0C and 1000 rpm. Electrospinning parameters for PMMA are adjusted as 120 mm nozzle to collector distance, 25 kV voltage, 3.5 mL/h flow rate. The total 10 mL PMMA solution is electrospun on aluminium foil then the mat is removed.

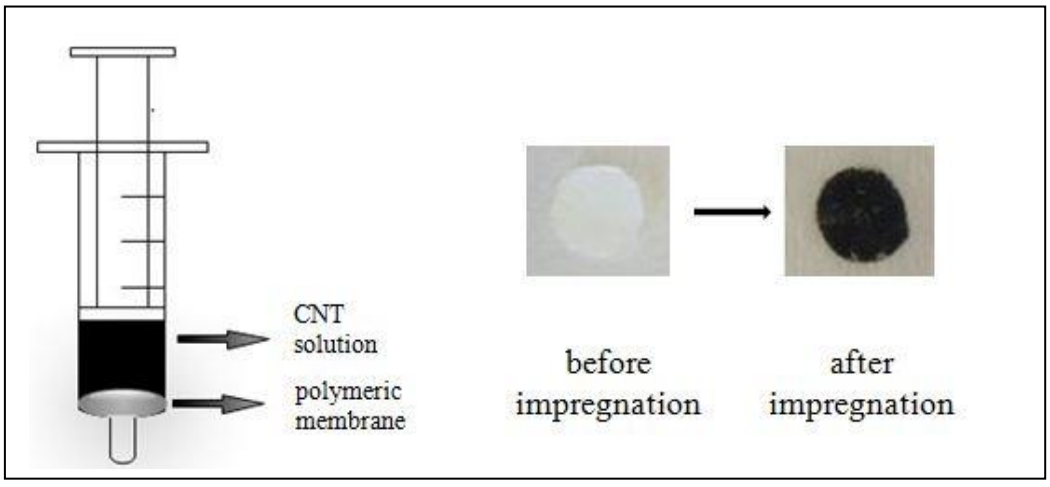

Figure 2.2 Impregnation Process of Polymer Membrane

For the fabrication of sensor chips, all three type polymer mats are cut into circular pieces with a 0.9 cm diameter. PVDF, PS, and PMMA chips are carefully

placed at the bottom of 2 mL syringe one by one then 500 μL of 0.2, 0.1, 0.05, 0.025, and 0.012wt % MWCNT solutions are passed through each polymer membrane like filtration process. MWCNT impregnated membranes are kept under fume hood overnight until the whole water is evaporated.

2.4. Resistivity Measurement

The dried MWCNT impregnated polymer membrane is placed onto a glass slide and connected to the multimeter via two probe system having 0.5 cm aperture. The membrane is closed with a chamber to keep gas molecules of acetone and toluene inside the chamber. Needle of a 2 mL syringe is attached to the chamber. The software of multimeter is started and baseline is waited for stabilization for 2-5 minutes. After that a drop of acetone is injected and it gives a response by increasing resistivity. Thereafter saturation of the sensor occurs due to the solvent molecules, they are swept by air and decrease in resistivity is observed.

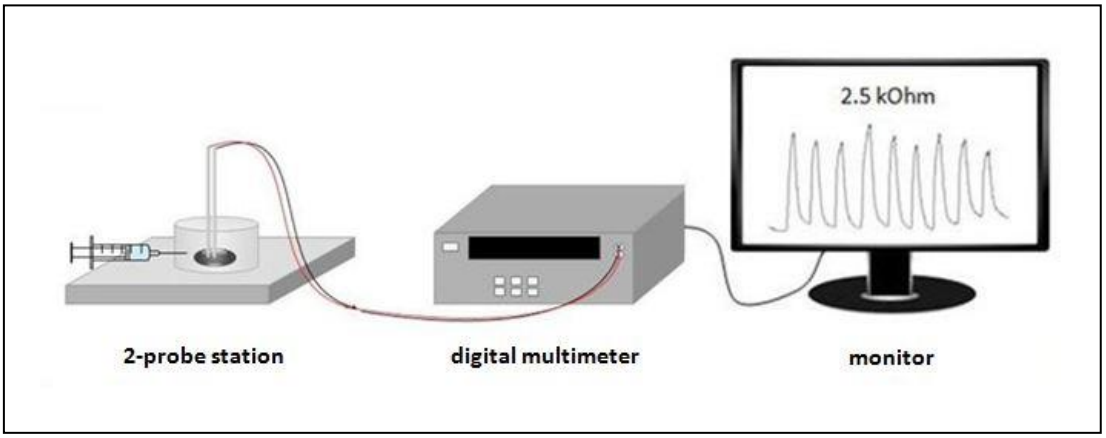

Figure 2.3 Two probe resistivity station and components

2.5. Fabrication of Microfluidic Chip

For the enhancement of stability of sensors, microfluidic chip is designed. The components of microfluidic chip are illustrated in figure x. PMMA sheet with a 2 mm thickness is used as sensor platform and the sensor is stabilized onto that platform by double-sided adhesive. Two copper electrodes are then placed on the sensor and this system is covered by PMMA sheet.

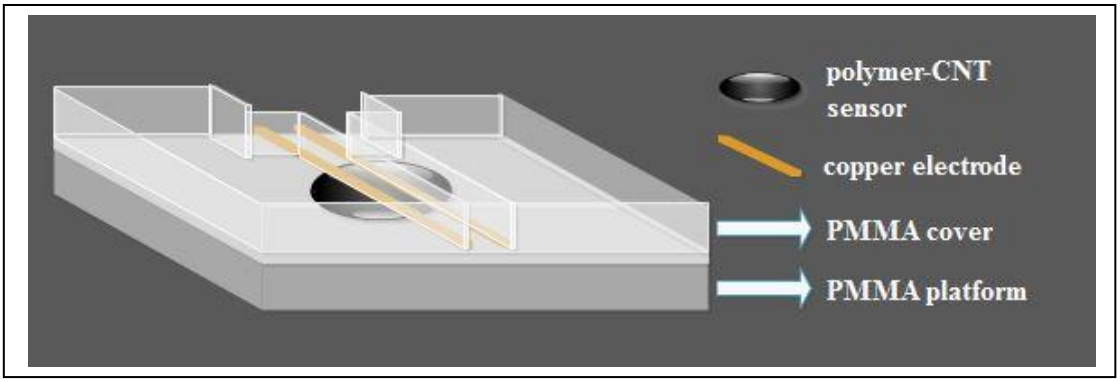

Figure 2.4 Components of microfluidic sensor chip

To obtain the optimum conditions for working of sensor, three different designs are fabricated. PMMA platform is held constant in each prototype, yet shape of PMMA cover and width of copper electrodes are changed. Figure 2.5 shows the three prototypes and their varieties.

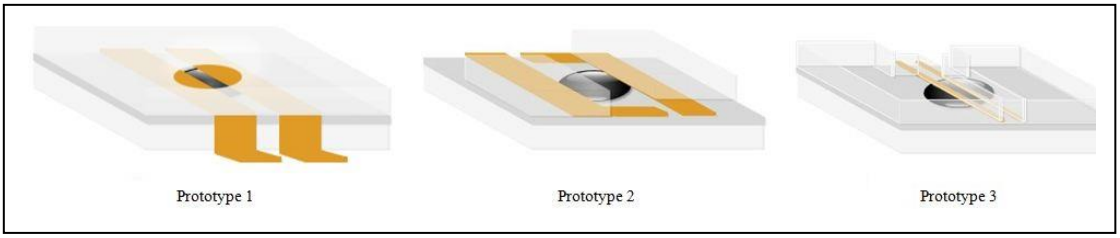

Figure 2.5 Three different designs for microfluidic chip

CHAPTER 3

RESULTS & DISCUSSION

3.1. Characterization and Fabrication of Sensor Interface

Electrospun poly(vinylidene fluoride) (PVDF), polystyrene (PS), and poly(methyl methacrylate) (PMMA) nanofibers were characterized by Scanning Electron Microscopy (SEM). The characterization of carbon nanotube solution was performed by pH meter and sensor characterization was obtained by multimeter and SEM.

3.1.1. PVDF, PS, and PMMA Nanofibers

All three polymeric mats were obtained by electrospinning technique. The several parameters have been carefully adjusted to control the morphology of product. Table 3.1. shows the optimum parameters for each polymer. By varying these parameters, not only morphology but also diameter of fibers were manipulated, PVDF, PS, and PMMA fibers were utilized as sensor platform.

Table 3.1. Electrospinning parameters of PVDF, PS, and PMMA

polymer	solution conditions		spinning conditions		
	concentration (wt%)	solvent composition by volume	spinning distance (mm)	voltage (kV)	flow tare (mL/h)
PVDF	25	DMF(4):Acetone(1)	145	23	3
PS	15	DCM(4):DMF(1):Acetone(1)	120	25	3.5
PMMA	20	DMF	210	25	3.5

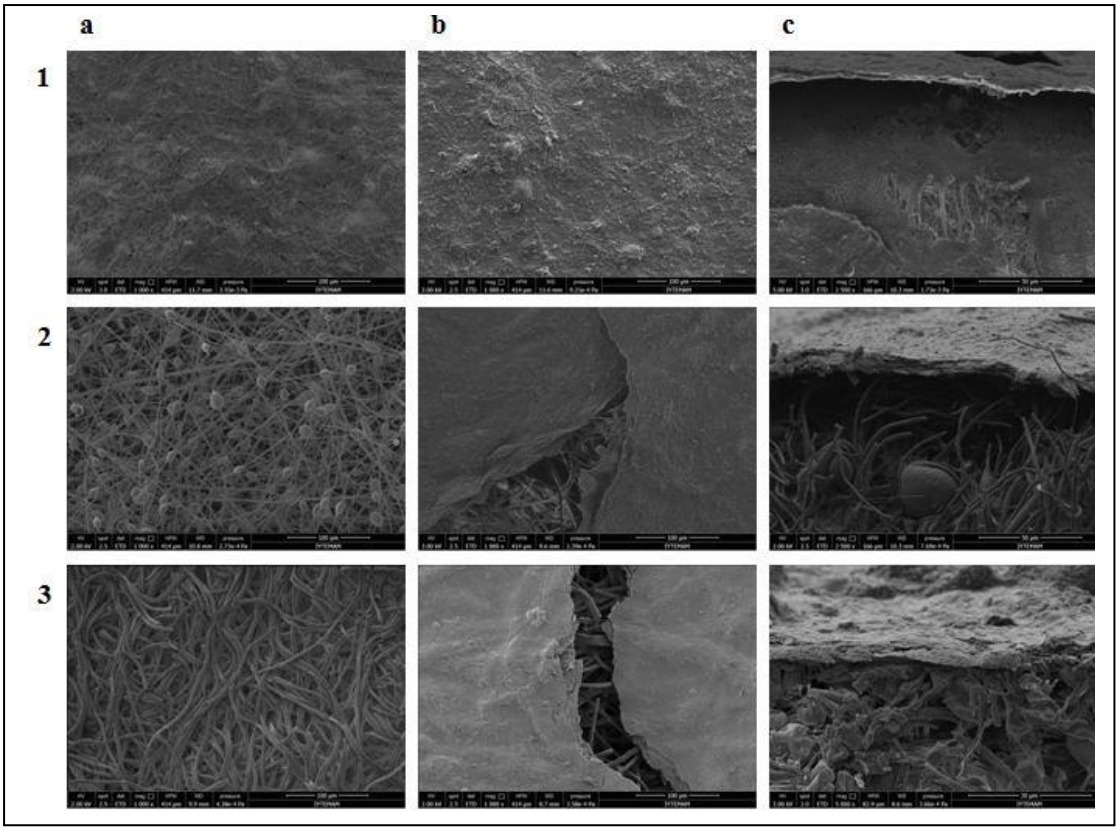

Figure 3.1 SEM images polymer fiber (a), polymer- CNT composite (b), and side view of composite (c) of PVDF (1), PS (2), and PMMA (3)

Figure 3.1 shows SEM images of morphology of pristine polymers and polymer-CNT compositions. The pristine PVDF, PS, and PMMA fibers are shown in column a. The diameters of PVDF fibers were found to be thinner as compare to PS and PMMA. This makes PVDF mat is very tough and therefore it exhibits paper like feature. The film like morphology facilitates CNTs impregnation onto the surface. The other fibrous or fibrillar structures or thin membranes are spoiled during impregnation process due to low mechanical properties. Therefore instead of perfect fiber structure a mixed morphology of fiber and film in PVDF membranes was experienced suitable for CNT impregnation. On the other hand the wool-like form of PS and PMMA mats, with higher diameter relative to PVDF, can also hold CNTs on the surface by the overlapped fibers.

Column b shows the SEM images of polymer CNT composite. The cracks with various sizes in CNT network are typically defect on surface. The detailed image analysis of column b (The scale bar shows 100 μm) indicates that PS and PMMA membranes cause larger cracks due to their soft and easily deformable structure which lowers mechanical strength. During impregnation of CNT solution

some portion of CNTs are deposited onto the membranes but some of them (small sized <400 nm) penetrate beneath the surface. That creates uneven distribution of CNT network and rough morphology in composite material with larger sized and amount of cracks. However; toughness and paper-like morphology of PVDF membranes result in smooth surface thus, crack size of PVDF is approximately 5 fold smaller than that of PS and PMMA. Column c is the side view of fiber-CNT mats. CNT layer thicknesses were found to be that 3.5, 8.4, and 5.6 μm for PVDF, PS, and PMMA, respectively.

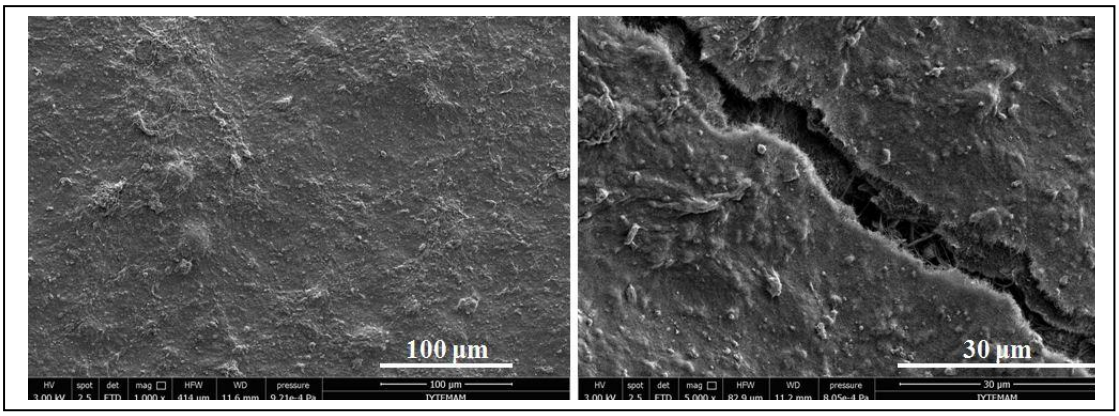

Figure 3.2 SEM images of PVDF-CNT composite with 100μm (left) and 30μm (left)

3.1.2. Carbon Nanotube (CNT) Solution

As stated above carbon nanotubes (CNTS) have employed to fabricate conductive layer. The impregnation has performed by applying CNT solution onto the polymer membranes. Five different CNT concentrations, 0.2wt %, 0.1wt %, 0.05wt %, 0.025wt %, and 0.012wt %, are tested for to optimize the best condition. The solution conductivity of each solution was quantified. Figure 3.3 shows the relation between conductivity and concentration of CNT solution. A gradual increase in conductivity was observed clearly with an increasing concentration. The conductivities were found to be that 9.9, 15.7, 29.4, 56.6, and 121.5 μS/cm for 0.012%, 0.025%, 0.05%, 0.1%, and 0.2%, respectively. The linear behavior of conductivity-concentration dependency provides control over solid state conductivity.

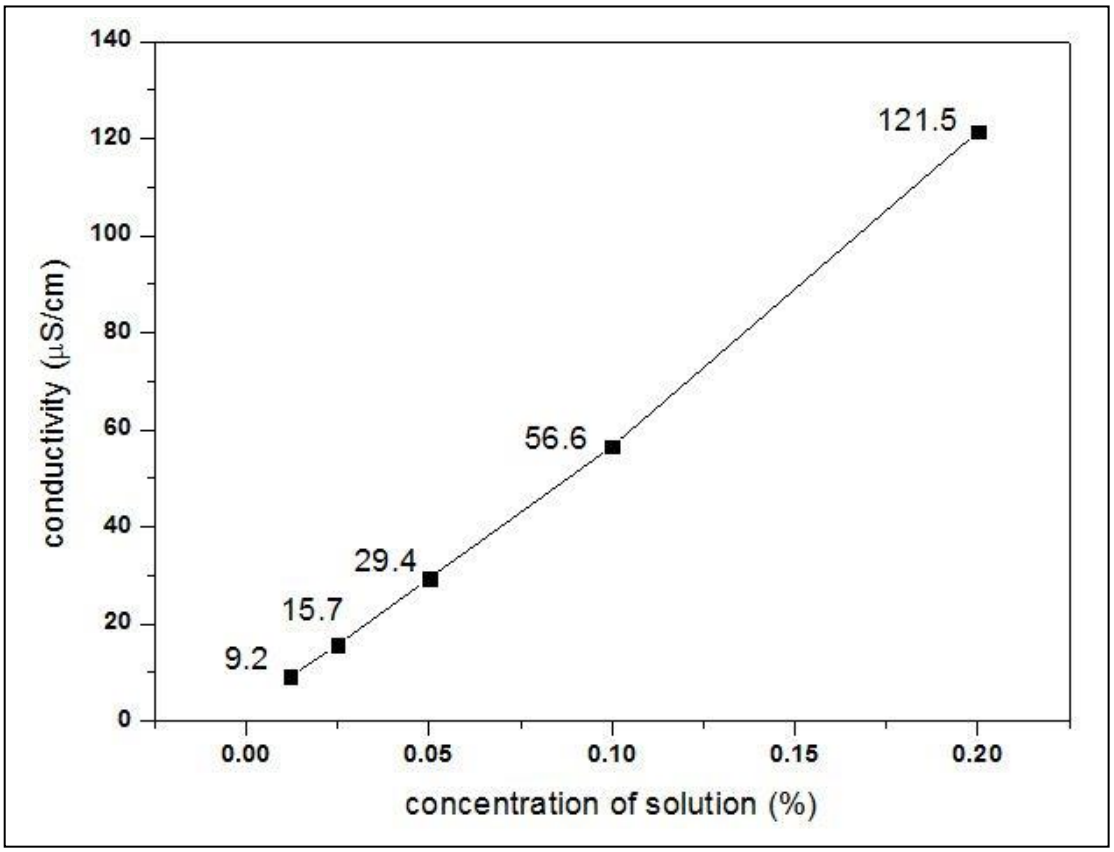

Figure 3.3 The graph of concentration vs. conductivity of CNT solution

3.1.3. Solid State Conductivity of Polymer Membranes

To explore the resistivity behavior of each polymer membrane, resistivity measurement was performed by multimeter. Figure 3.4 shows the resistivities of polymer membranes prepared by using 5 different conditions (0.012%, 0.025%, 0.05%, 0.1%, and 0.2%). Here and after we call polymer membrane – CNT composite as "sensor". The figure 3.4 shows the images of 5 different sensors. The color of sensors is getting dark from left to right due to the increasing in impregnated CNT solution. Conversely, resistivity of sensors decreases in same direction. Impregnation with a higher concentration of CNT solution leads to deposit more carbon nanotubes on the membranes. Consequently, more conductive sensors can be obtained with higher concentration of CNT solution. This characteristic helps to control the resistivity of sensor depending on requirement. As summarized at table 3.2. solution conductivity of CNT solution and solid state resistivity of sensors are

inversely proportional as expected. The resistivity behavior of sensors exhibit two zones. At zone I, resistivity changes with increasing CNT concentration are much steeper than zone II. This considers that as solution concentration increases above 0.05% impregnation efficiency reaches to limit value that yield total coverage of surface. Therefore resistivity changes slowly and monotonously with respect to zone I. In other words, 0.05%is a threshold for 2-2.5 kOhm solid state resistivity.

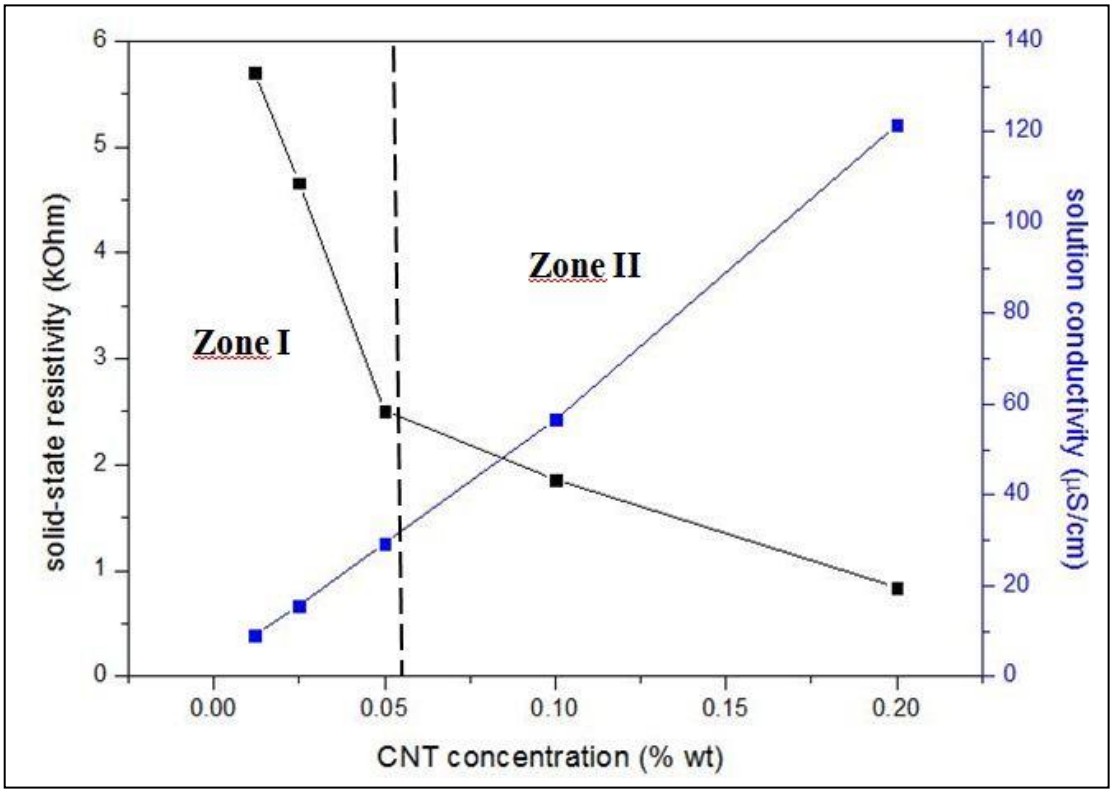

Figure 3.4 Change in resistivity of sensors and conductivity of CNT solution with different solution concentration

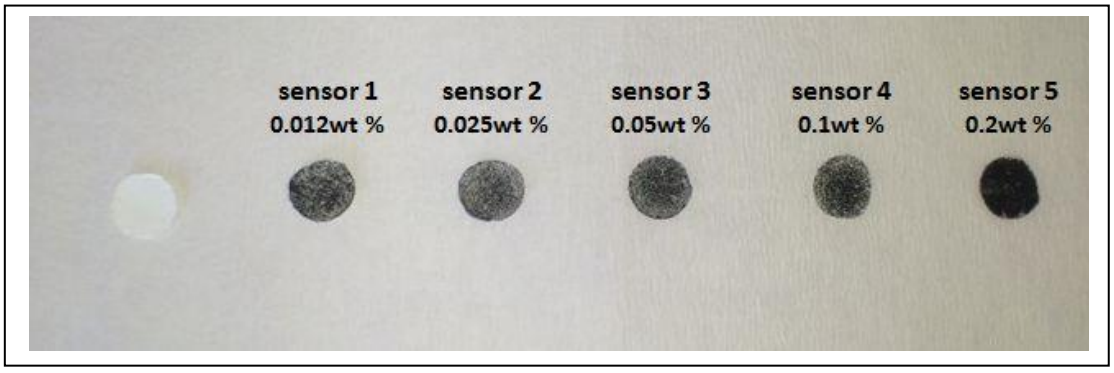

Figure 3.5 Images of PVDF sensor with increasing CNT concentration

Table 3.2. Properties of five different PVDF sensors

sensor name	CNT solution concentration (wt %)	CNT solution conductivity (μS/cm)	sensor resistivity (kOhm)
Sensor 1	**0.012**	**9.2**	**5.70**
Sensor 2	**0.025**	**15.7**	**4.66**
Sensor 3	**0.05**	**29.4**	**2.51**
Sensor 4	**0.1**	**56.6**	**1.86**
Sensor 5	**0.2**	**121.5**	**0.843**

The results of solid state resistivity of sensors indicate that 0.05% and above concentrations provide desired base resistivity for gas sensing. Therefore 0.05wt% and 0.1wt%CNT solutions were used to fabricate PVDF, PS, and PMMA sensor chips.

3.2. Determination of Behavior of PVDF-PS-PMMA Sensors

To explore the potential of utilization of sensors for pre-diagnosis of diabetes and lung cancer, the all sensors are exposed to acetone and toluene, respectively and the response of sensors monitored and resistivity change recorded. To understand effect of acetone and toluene on the sensors, real time responses are firstly obtained from PVDF, PS, and PMMA sensors. Stability of each sensor is then investigated. Furthermore, limit of detection (LOD) and dynamic range of the three sensors with various concentrations of acetone and toluene are determined to indicate whether working region of sensors is encompassed by concentration of target gases of healthy and patient individuals.

3.2.1. Real Time Responses of PVDF, PS, and PMMA Sensors

Real time analysis provides to observe online performance of sensors. Here the VOC compound is purged into gas chamber and swept several times.

Figure 3.6 shows the typical resistance responses, $\Delta R/R_b$ (ΔR: resistivity change and R_b: baseline resistivity) of PVDF sensor to acetone and toluene. Adsorption and desorption characteristic of the sensor indicates that Langmuir

isotherm type increase and response for both acetone and toluene gases exist. Acetone exhibit a ~27 % change in resistivity; however toluene causes a ~10 % change in resistivity. The stability and reproducibility is good enough to rely on response of PVDF sensor. In each trial, same resistivity change is observed with respect to quantity and behavior of adsorption and desorption.

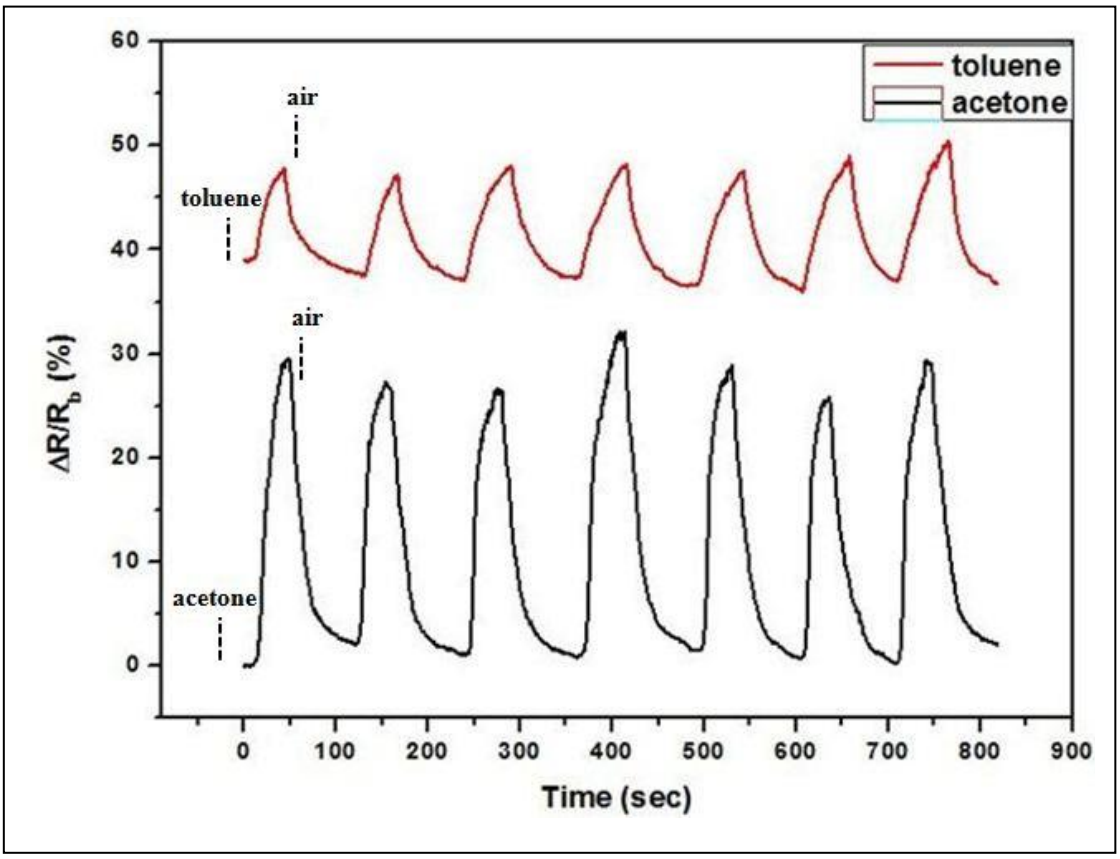

Figure 3.6 Acetone and toluene response (ΔR: resistivity change and R_b: baseline resistivity) of PVDF sensor

The figure 3.7 shows the behavior of PS sensor upon acetone and toluene exposure. Comparing to PVDF sensor the reproducibility, response, and recovery are poor. Signal-to-noise ratio is also relatively lower due to instability issues. The soft and wool-like nature of polystyrene makes it more fragile thus PS membrane can be easily affected by external mechanical forces. During measurement by probe station, the probes deforms PS sensor and therefore causes instability in PS sensor. Acetone and toluene exposure changes resistivity ~3.48 % and ~5.98 %, respectively.

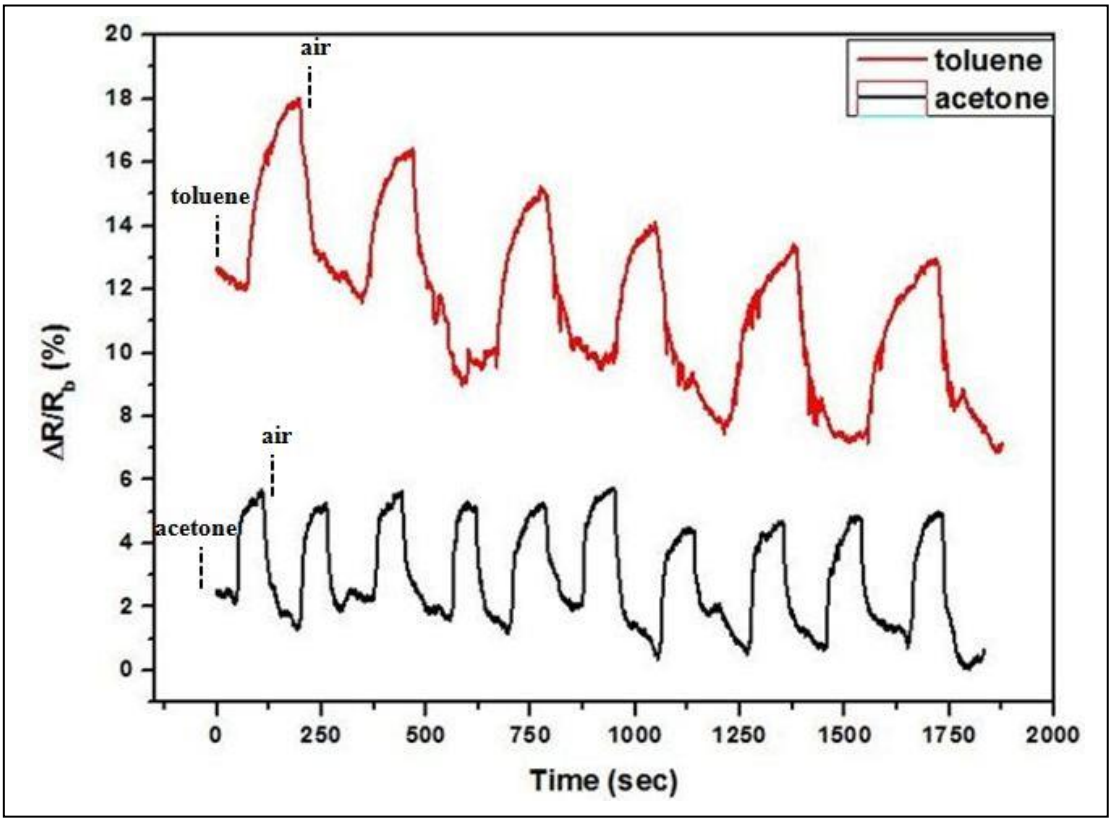

Figure 3.7 Acetone and toluene response (ΔR: resistivity change and R_b: baseline resistivity) of PS sensor

The similar investigation for PMMA sensors has been investigated. PMMA sensor chips exhibit moderately high quality response with respect to PS sensors. However; baseline acquisition emerged as a common difficulty for PMMA sensors. Its reproducibility to both acetone and toluene is in an acceptable range despite of fluctuation in baseline.

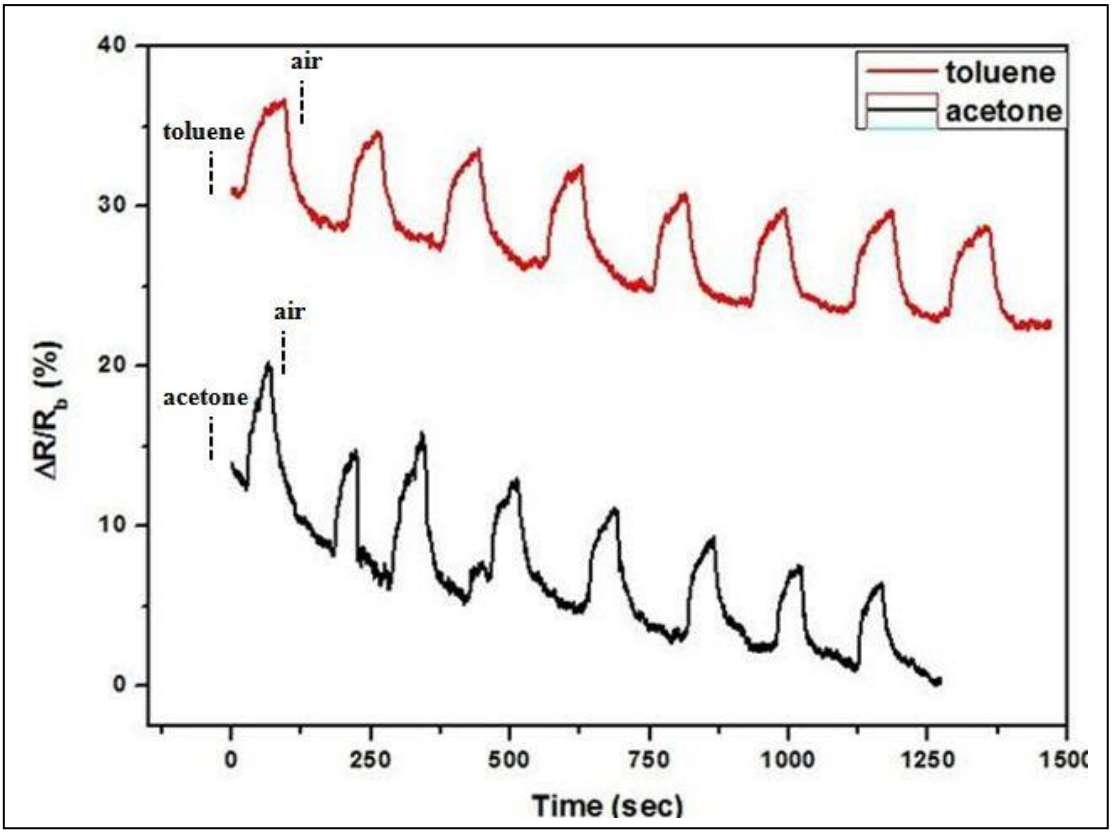

Figure 3.8 Acetone and toluene response (ΔR: resistivity change and R_b: baseline resistivity) of PMMA sensor

Table 3.3. Percent responses of three sensors to acetone and toluene

sensor type	acetone response %	toluene response %	acetone: toluene ratio
PVDF	**27**	**10**	**2.7**
PS	**3.48**	**5.98**	**0.6**
PMMA	**6.41**	**6.24**	**~1**

Table 3.3. indicates responses of PVDF, PS, and PMMA sensors. They have different selectivity to acetone and toluene. The characteristics of polymers that are constituents of sensor significantly affect their responses. For example, the acetone to toluene ratio is higher in PVDF sensor thus it means PVDF sensor is more selective to acetone. The opposite situation occurs in PS sensor and makes it selective to toluene. However; there is no significant distinction in PMMA sensor. This is caused by conformational change on carbon nanotube network. If target gas molecule is the theta solvent of that polymer, change in resistivity is greater than non-solvent of polymer. This behavior can be explained by reactive adsorption of gas molecules on fibers. When a fiber is exposed to its theta solvent, polymer first begins to swell in

some extent then causes deformation on upper layer that increases the number of micro-sized cracks on CNT network and resistance to electron flow occurs.

3.2.2. Responses of Sensors to Various Concentrations of VOCs

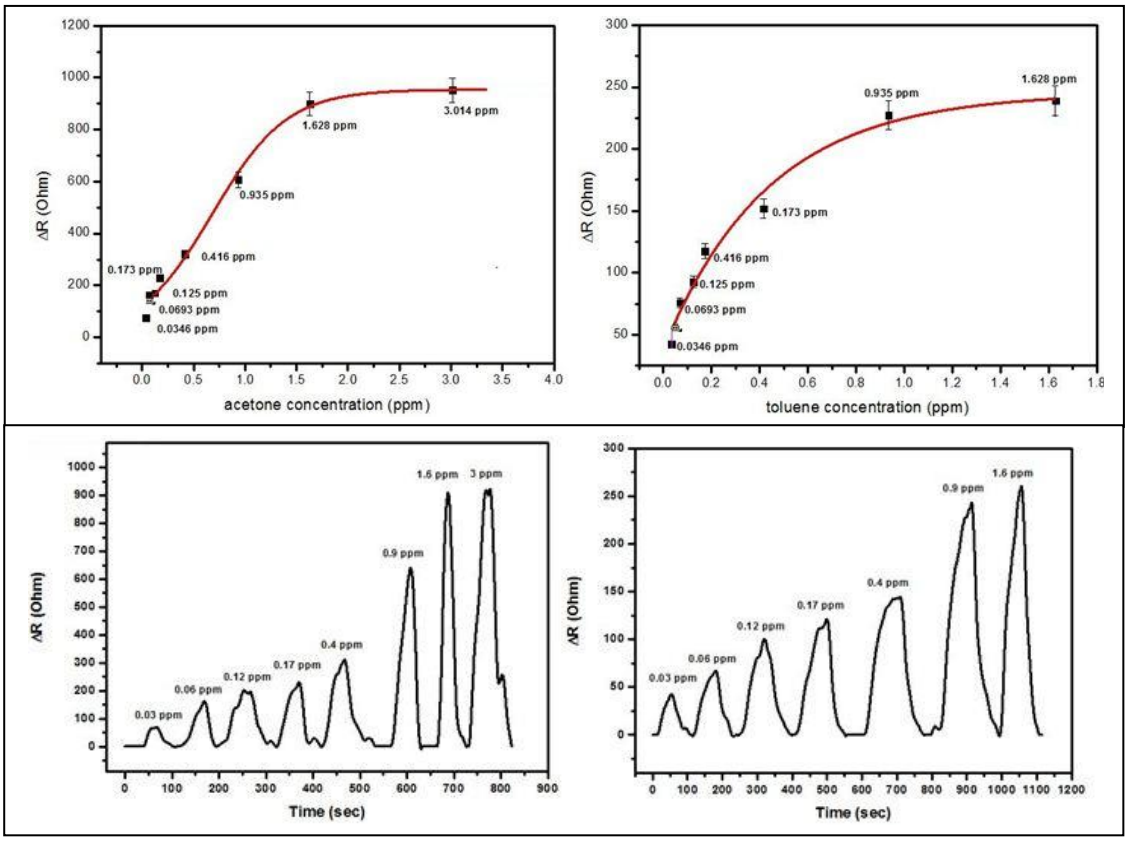

Figure 3.9 Responses of PVDF sensor to various acetone (left) and toluene (right) concentrations

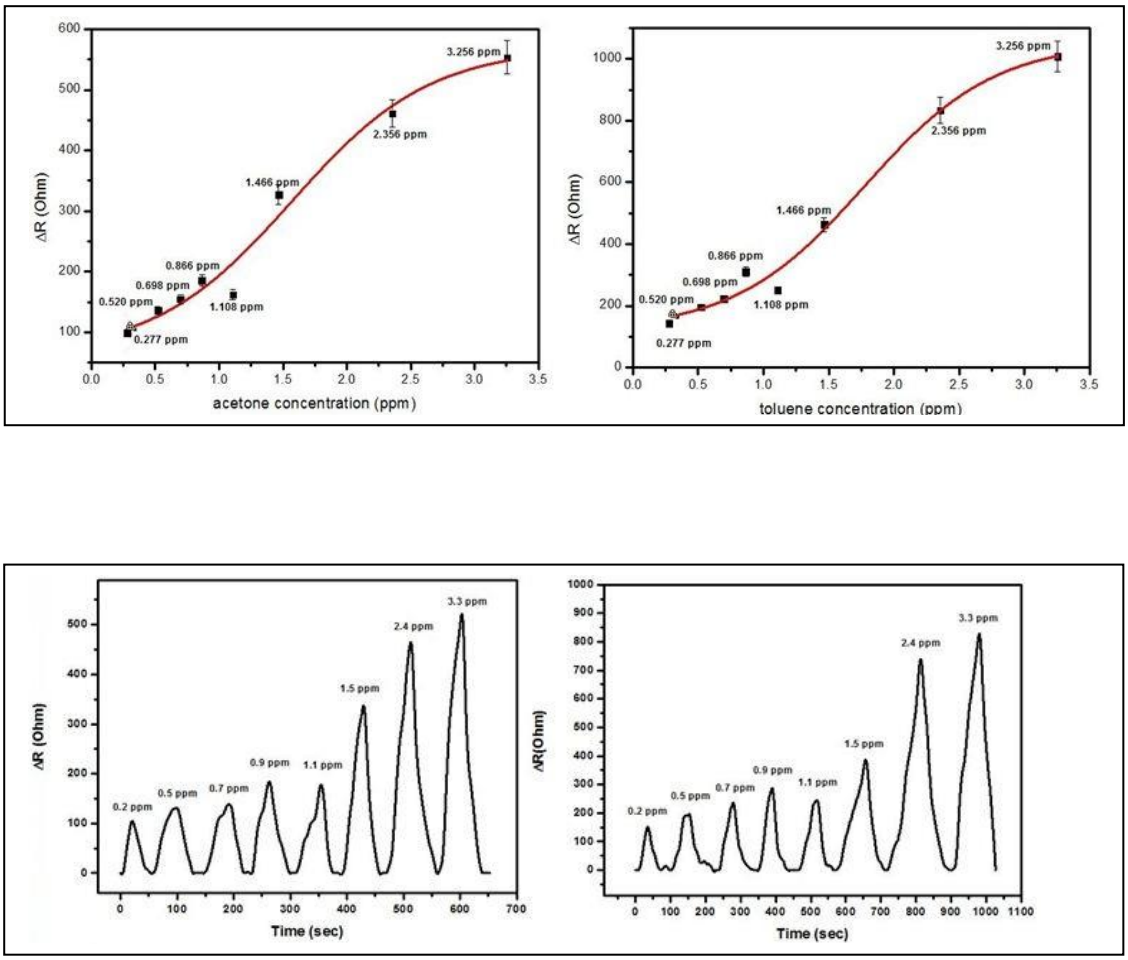

Figure 3.10 Responses of PS sensor to various acetone (left) and toluene (right) concentrations

Concentration screening of VOCs have been performed for PVDF sensor platforms. Since concentrations of acetone and toluene is very low in breath as mentioned at the beginning of the thesis. Detection limits of PVDF, PS, and PMMA sensors are 0.0346, 0.277, and 0.0278 ppm, respectively. The LOD level of our sensor platform is in the range of diagnostics as compare to literature.

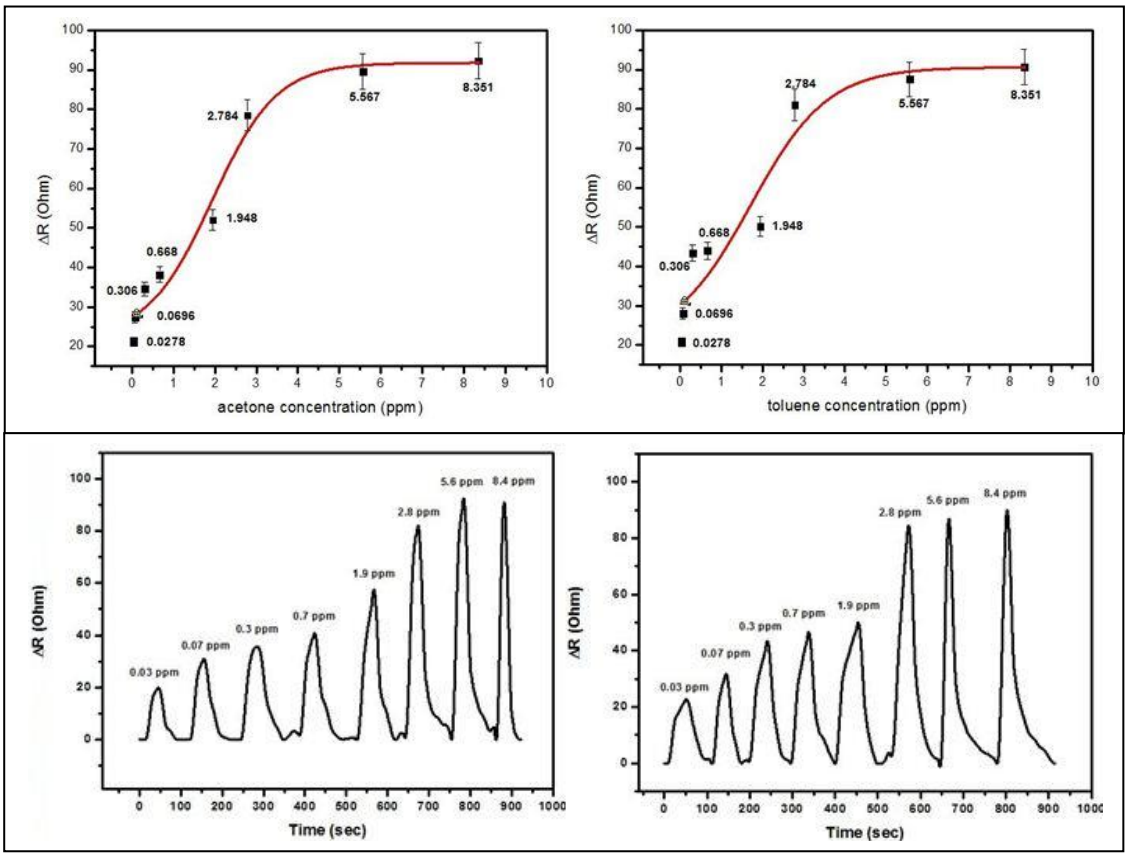

Figure 3.11 Responses of PMMA sensor to various acetone (left) and toluene (right) concentrations.

3.2.3. Reusability Analysis of Sensors

Reusability test is perfomed for each sensor by the exposure of acetone vapor. The behaviour of PVDF sensor to seventy times acetone exposure is investigated. The sensor retains ~60% of its original activity. However; the sixtyfive times exposure increases instability and fluctuation of PS sensor.

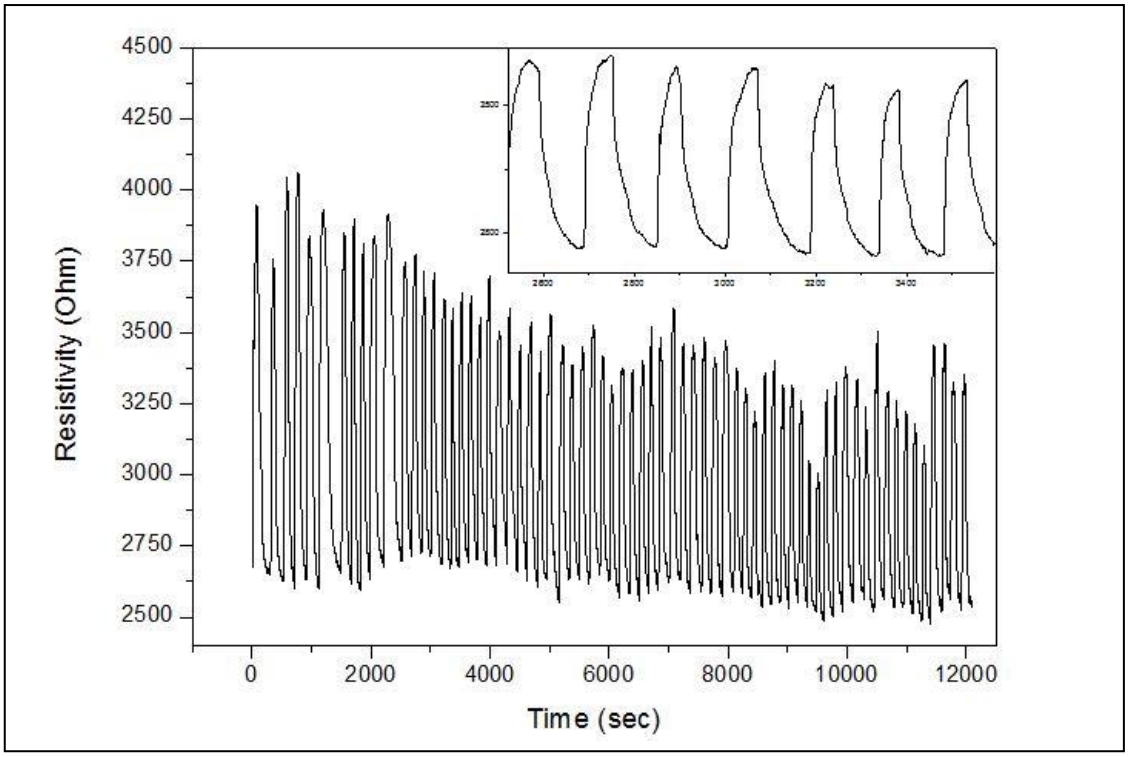

Figure 3.12 Reusability of PVDF sensor

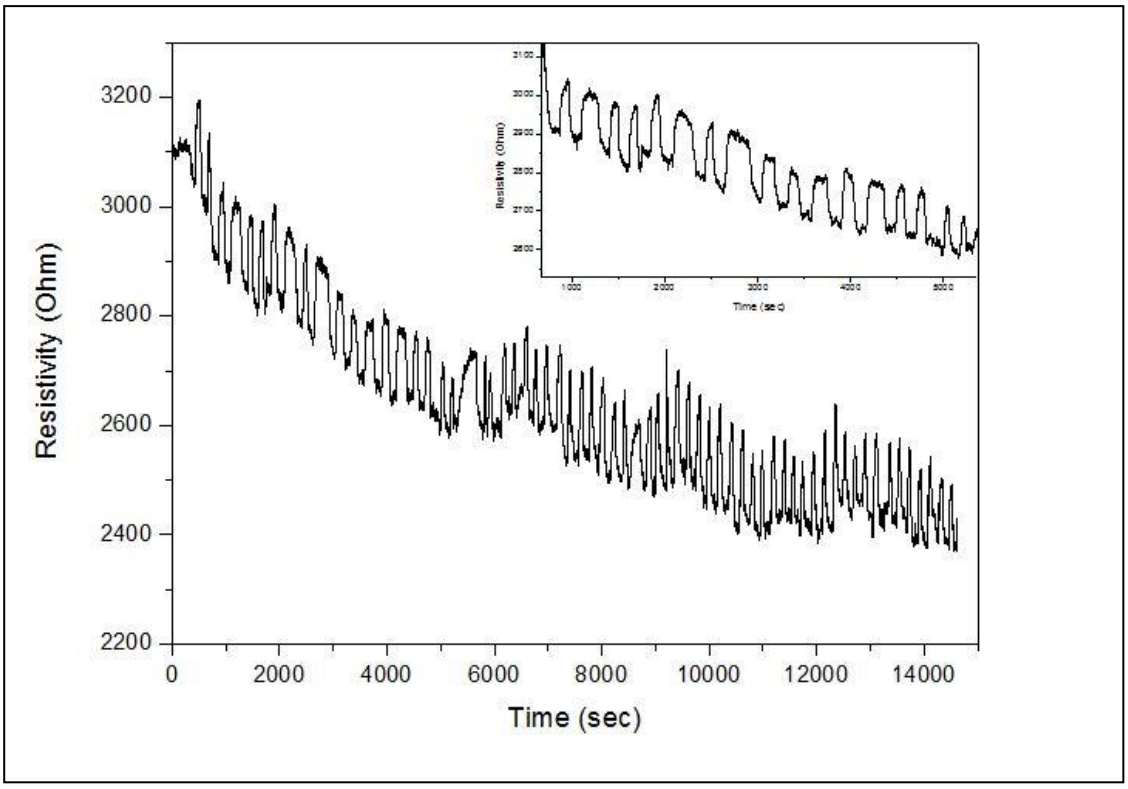

Figure 3.13 Reusability of PS sensor

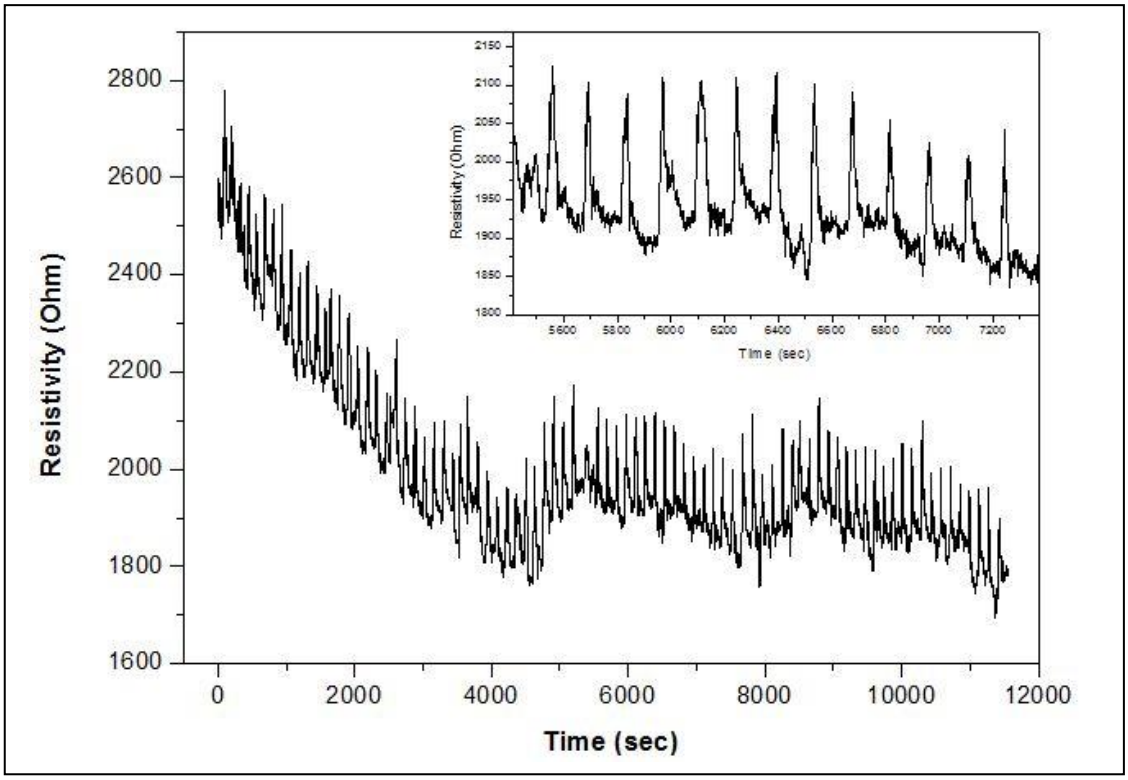

Figure 3.14 Reusability of PMMA sensor

CHAPTER 4

BREATH ANALYSER

Continuous monitoring of health status is a common medical practice for in patient's conditions that often requires wiring instruments to patients. As a part of future medicine and preventive healthcare concept, there is growing tendency disseminating available and advancing continuous monitoring technology for outpatients. However bulky instruments, power requirements, difficulties in data transfer limit the applicability of current settings. The portable/wearable sensing devices are getting employed for monitoring some diseases such as Chronic Obstructive Pulmonary Disease (COPD). These concept devices provide suitable platform for COPD patients to monitor lung functions for diagnosis and treatment. There are examples of miniaturized respiratory instruments such as mobile peak-flow meters, spirometers that are low cost point of care phone-powered prototypes. Common approach of prototype devices usually concentrated around the idea of count of turns of mini-turbines yielding noncorrelating breath count.

We here present new sensor device utilizing carbon nanotube impregnated paper based sensing interface that captures exhaled breath. The device has simplistic design that detects resistivity change upon encountering breath. This study benefits from exhaled breath for another medicinal application; it is aimed to fabricate a disposable sensor platform for investigation of lung function like spirometer.

New generation wearable biosensors hold great promise for monitoring health status and provide allowing early-stage intervention, reducing healthcare costs and improving quality of life. The thin film nanomaterial based biosensor, ultra-light weight batteries and wireless communication platforms facilitate miniturazation process. We propose a new microfluidic cartridge coupled nanofiber impregnated nanotube sensors, designed for a diverse range of stimuli. These sensors can provide the flexibility, sensitivity, specificity and autonomy required for future technology. The sensor response is electrochemical, with a detectable signal that allows non-experts to operate the sensor without additional equipment. To demonstrate the

potential of the concept we have chosen as primary focus to develop breath counter for continuous diagnostics, amenable to low-cost mass production. We foresee that diseases such as Chronic Obstructive Pulmonary Disease (COPD) can be monitored by proposed portable breath counter.

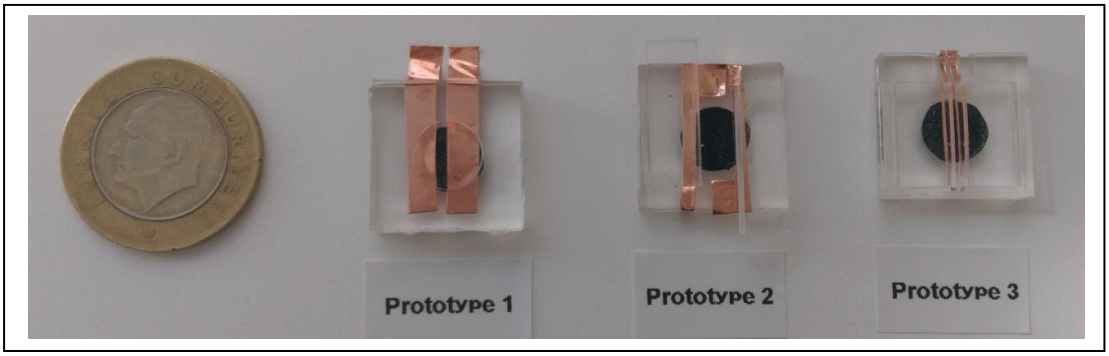

Figure 4.1 Photographs of the microfluidic chip prototypes

Nanofiber platforms made of poly(vinylidene fluoride) were impregnated by CNT were shown in Fig.1. Electron microscopy images of pristine nanofiber platform and after CNT impregnation indicates that nanotubes were accumulated as thick layer and evenly distributed (see Fig. 2).

Poly methyl methacrylate (PMMA) microchannels were assembled as multilayer configuration that composed of four layers: 1) PMMA base, 2) nanofiber-CNT electrochemical membrane 3) conductive metal tape 4) PMMA microfluidic channel. This whole structure is called as microfluidic cartridge (μ-cart) here and thereafter. The schematic 1 shows the prototype design of μ-cart. μ-cart was designed to collect maximum amount of exhaled breath by means of large opening in front face that directing breath to the CNT impregnated nanofiber membrane. The dimensions of conductive tapes were intentionally varied to test the effect of accumulation of charge. The μ-cart prototypes 1, 2 and 3 were shown in Fig. 3.

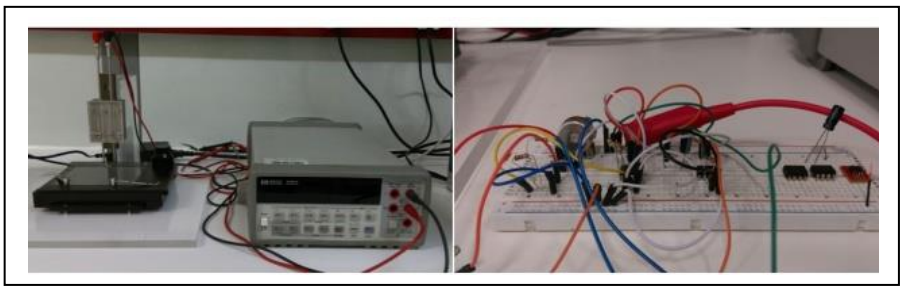

Figure 4.2 Agilent 34401A bench multimeter electrochemical station (left) and circuit design (right)

The initial electrical characterization has been performed by Agilent 34401A bench multimeter electrochemical station. For resistivity variation measurements each cartridges were fixed pressure controlled metal holders.

Upon exhaled breath each prototypes have responded by resistivity change. The prototype 1 exhibited non-correlating response for breath pulses (exhaled breath applied to the cartridge from fixed distance: 10 cm), while prototype 2 showed weak resistivity changes for breath test (see top graph in Fig. 5.). The reproducible resistivity change upon exhaled breath has provided by prototype 3. By utilizing the circuit given in Fig. 7, the voltage variation using bench multimeter was also measured. The change in potential was monitored by the same setup for identical cartridges prototype 1 to 3 in Fig. 5, middle graph. The correlation between exhaled breath pulses and potential change were found to be solely positive for prototype 3.

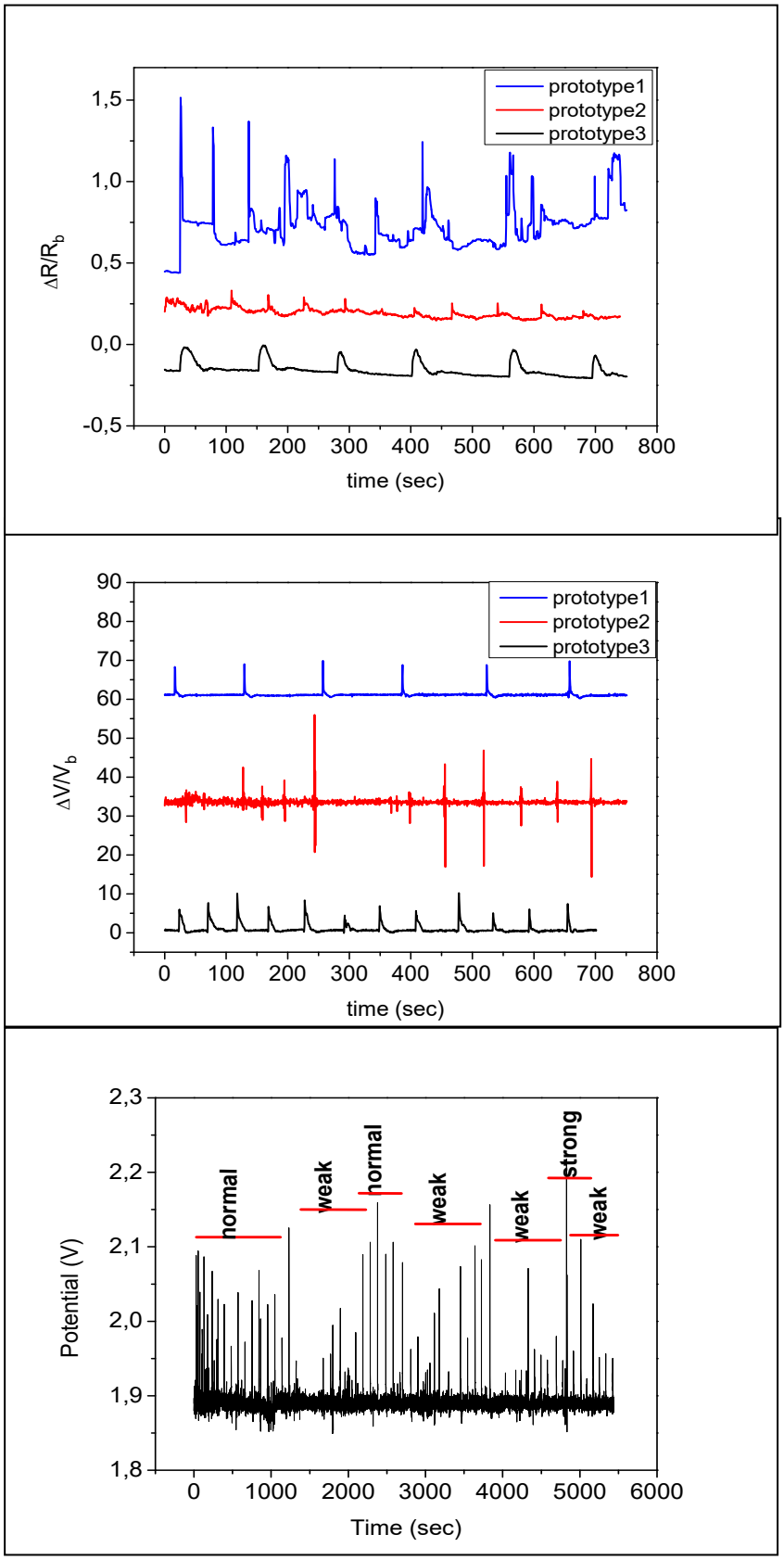

Figure 4.3 Resistivity changes of prototype cartridges 1, 2 and 3 (top graph), Potential change of prototype cartridges 1, 2 and 3 (middle graph), Potential change versus time graph of prototype 3 cartridge (bottom graph)

The prototype 3 have been employed for several exhaled breath scenario: normal and weak breathing cycles followed by very weak breathing and very strong breathing (see Fig. 5, bottom graph, weak and strong breathing have been applied by adjusting the distance between experimenter and cartridge, 10 cm distance were assumed to be optimum distance). The μ-cart prototype 3 were further used to developed portable device.

After validation trials, miniaturization steps have been taken. The portable device prototype, were shown in Fig. 9, is hand held device that is sensitive to resistivity changes. The hand held device is composed of three components which are μ-cart integrated circuit board, electronic interfacing circuit and LCD display. The validation experiments were performed by exhaled breath test that monitor the change in potential over the time. The measured potential differences were found to be 0.1 to 2.9 V (max and min detectable signals in Fig. 9). This results shows that μ-cart integrated device is sensitive that detects weak and strong exhaled breath.

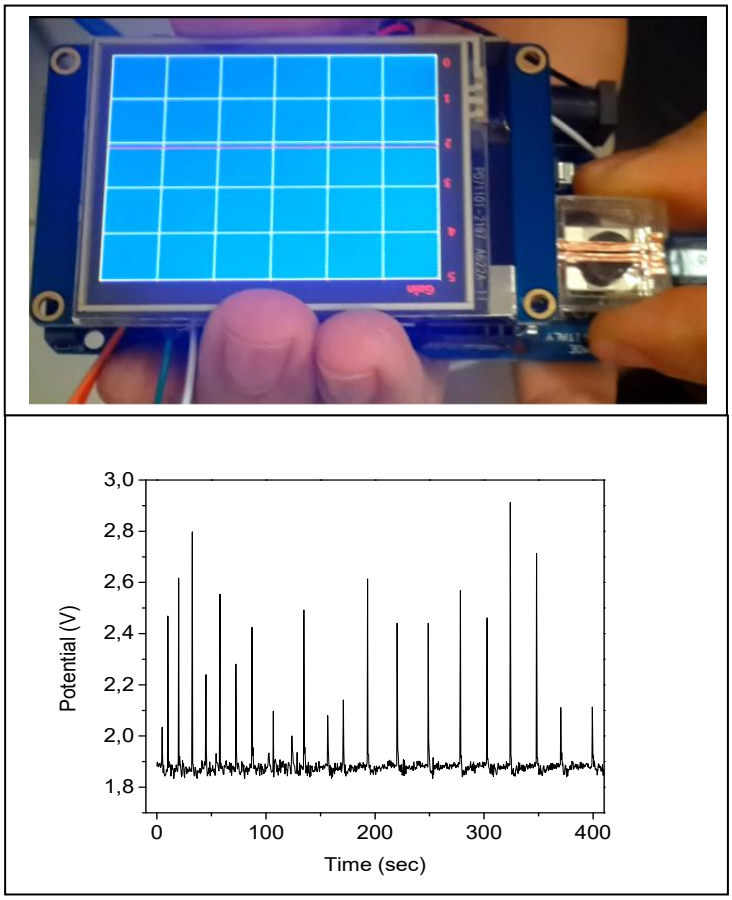

Figure 4.4 Circuit design (top), Potential change of prototype hand held device (bottom)

CHAPTER 5

CONCLUSION

We described fabrication of polymer nanofiber supported multi walled carbon nanotube composite electrode as a sensor platform for monitoring diabetic biomarker “acetone” and lung cancer biomarker “toluene” in exhaled breath. The sensor platform is made of two layers, polymeric nanofiber mat and physically assembled multi walled carbon nanotubes. The polymer nanofiber mats were fabricated by electrospinning of Poly(vinylidene fluoride) (PVDF), polystyrene (PS), and poly(methyl methacrylate) (PMMA) and then aqueous solution of well-dispersed MWCNTs with ~120 μS/cm solution conductivity were filtered through the mats yielding a micrometer thick nanotube layer. The gas sensing capabilities of sensor platforms were validated by controlled acetone and toluene exposure. The PVDF nanofiber supported sensor exhibited enhanced response to acetone between 35 ppb to 3.0 ppm due to acetone specific reversible swelling of nanofiber with respect to other two platforms. On the other hand PS and PMMA supported sensors showed response to ethanol between 270 ppb to 3.0 ppm and 27ppb and 8.1 ppm respectively. Toluene responses were studied by using same configuration of sensors of PVDF (30ppb-1.4ppm), PS (270ppb-3.2ppm) and PMMA (27ppb-8.3ppm).

In further studies, new electrode was assembled in micro chamber that provide efficient sample capturing. Moreover new portable breath analyser was also utilized to facilitate VOC monitoring. The portable device was validated with real samples that show good selectivity to acetone.

REFERENCES

Amann, A., W. Miekisch, J. Schubert, B. Buszewski, T. Ligor, T. Jezierski, J. Pleil, and T. Risby. 2014. "Analysis of exhaled breath for disease detection." *Annu Rev Anal Chem (Palo Alto Calif)* 7:455-82. doi: 10.1146/annurev-anchem-071213-020043.

Ayala, Antonio, Mu, #xf1, Mario F. oz, Arg, #xfc, and Sandro elles. 2014. "Lipid Peroxidation: Production, Metabolism, and Signaling Mechanisms of Malondialdehyde and 4-Hydroxy-2-Nonenal." *Oxidative Medicine and Cellular Longevity* 2014:31. doi: 10.1155/2014/360438.

Broza, Y. Y. , and H. Haick. 2013. "Nanomaterial-based sensors for detection of disease." *Nanomedicine* 8 (5):785-806.

Broza, Y. Y., P. Mochalski, V. Ruzsanyi, A. Amann, and H. Haick. 2015. "Hybrid volatolomics and disease detection." *Angew Chem Int Ed Engl* 54 (38):11036-48. doi: 10.1002/anie.201500153.

Buszewski, Bogusław, Joanna Rudnicka, Tomasz Ligor, Marta Walczak, Tadeusz Jezierski, and Anton Amann. 2012. "Analytical and unconventional methods of cancer detection using odor." *TrAC Trends in Analytical Chemistry* 38:1-12. doi: 10.1016/j.trac.2012.03.019.

Cozza, Erika Simona, Orietta Monticelli, Enrico Marsano, and Peggy Cebe. 2013. "On the electrospinning of PVDF: influence of the experimental conditions on the nanofiber properties." *Polymer International* 62 (1):41-48. doi: 10.1002/pi.4314.

Garg, K., and G. L. Bowlin. 2011. "Electrospinning jets and nanofibrous structures." *Biomicrofluidics* 5 (1):13403. doi: 10.1063/1.3567097.

Greiner, A., and J. H. Wendorff. 2007. "Electrospinning: a fascinating method for the preparation of ultrathin fibers." *Angew Chem Int Ed Engl* 46 (30):5670-703. doi: 10.1002/anie.200604646.

Hakim, Meggie, Yoav Y. Broza, Orna Barash, Nir Peled, Michael Phillips, Anton Amann, and Hossam Haick. 2012. "Volatile Organic Compounds of Lung Cancer and Possible Biochemical Pathways." *Chemical Reviews* 112 (11):5949-5966. doi: 10.1021/cr300174a.

Halliwel, B. 1992. *Lab. Clin. Med.* 119:598.

Kaushik, Brajesh Kumar, and Manoj Kumar Majumder. 2015. "Carbon Nanotube: Properties and Applications."17-37. doi: 10.1007/978-81-322-2047-3_2.

Kim, Il-Doo, Seon-Jin Choi, Sang-Joon Kim, and Ji-Su Jang. 2015. "Exhaled Breath Sensors."19-49. doi: 10.1007/978-94-017-9981-2_2.

Kim, K. H., Shamin Ara Jahan, and Ehsanul Kabir. 2012. "A review of breath analysis for diagnosis of human health." *TrAC Trends in Analytical Chemistry* 33:1-8. doi: 10.1016/j.trac.2011.09.013.

Kittel, C. 1996. *Introduction to Solid State Physics*. Edited by J. Wiley. 7 ed. New York.

Konvalina, G., and H. Haick. 2014. "Sensors for Breath Testing From Nanomaterials." *Accounts of Chemical Research* 47 (1):66-76.

Lu, Xin, and Zhongfang Chen. 2005. "Curved Pi-Conjugation, Aromaticity, and the Related Chemistry of Small Fullerenes (<C60) and Single-Walled Carbon Nanotubes." *Chemical Reviews* 105 (10):3643-3696. doi: 10.1021/cr030093d.

Magniez, K., C. De Lavigne, and B. L. Fox. 2010. "The effects of molecular weight and polymorphism on the fracture and thermo-mechanical properties of a carbon-fibre composite modified by electrospun poly (vinylidene fluoride) membranes." *Polymer* 51 (12):2585-2596. doi: 10.1016/j.polymer.2010.04.021.

Nakhleh, M. K., H. Amal, H. Awad, A. Gharra, N. Abu-Saleh, R. Jeries, H. Haick, and Z. Abassi. 2014. "Sensor arrays based on nanoparticles for early detection of kidney injury by breath samples." *Nanomedicine-Nanotechnology Biology and Medicine* 10 (8):1767-1776. doi: 10.1016/j.nano.2014.06.007.

Poli, D., P. Carbognani, M. Corradi, M. Goldoni, O. Acampa, B. Balbi, L. Bianchi, M. Rusca, and A. Mutti. 2005. "Exhaled volatile organic compounds in patients with non-small cell lung cancer: cross sectional and nested short-term follow-up study." *Respir Res* 6:71. doi: 10.1186/1465-9921-6-71.

Salahuddin, S., M. Lundstrom, and S. Datta. 2005. "Transport effects on signal propagation in quantum wires." *Ieee Transactions on Electron Devices* 52 (8):1734-1742. doi: 10.1109/ted.2005.852170.

Skoog, D. , J. Holler, and S. Crouch. 1998. *Principles of Instrumental Analysis*. 6 vols, *Principles of Instrumental Analysis*. Canada: Thomson Brooks/Cole.

Smith, D., and P. Spanel. 2015. "SIFT-MS and FA-MS methods for ambient gas phase analysis: developments and applications in the UK." *Analyst* 140 (8):2573-91. doi: 10.1039/c4an02049a.

Tisch, U., and H. Haick. 2014. "Chemical sensors for breath gas analysis: the latest developments at the Breath Analysis Summit 2013." *J Breath Res* 8 (2):027103. doi: 10.1088/1752-7155/8/2/027103.

Wang, C., and P. Sahay. 2009. "Breath analysis using laser spectroscopic techniques: breath biomarkers, spectral fingerprints, and detection limits." *Sensors (Basel)* 9 (10):8230-62. doi: 10.3390/s91008230.

Zhang, M., and R. Baughman. 2011. "Assembly of Carbon Nanotube Sheets, Electronic Properties of Carbon Nanotubes."

Zhao, Zhizhen, Jingqing Li, Xiaoyan Yuan, Xiang Li, Yuanyuan Zhang, and Jing Sheng. 2005. "Preparation and properties of electrospun poly(vinylidene fluoride) membranes." *Journal of Applied Polymer Science* 97 (2):466-474. doi: 10.1002/app.21762.